NASA CR-62005
TE-12

CORRELATION OF INTERPLANETARY GEOMETRY WITH PROPULSION REQUIREMENTS FOR OPTIMAL LOW-THRUST MISSIONS

By Neal A. Carlson

February 1965

Prepared under Grant No. NsG-254-62 by
MASSACHUSETTS INSTITUTE OF TECHNOLOGY
Cambridge 39, Mass.

for

NATIONAL AERONAUTICS AND SPACE ADMINISTRATION

CORRELATION OF INTERPLANETARY GEOMETRY WITH PROPULSION REQUIREMENTS FOR OPTIMAL LOW-THRUST MISSIONS

by

NEAL ADRIAN CARLSON

B.S.E., Princeton University, 1962

SUBMITTED IN PARTIAL FULFILLMENT

OF THE REQUIREMENTS FOR THE DEGREES OF

MASTER OF SCIENCE AND

ENGINEER OF AERONAUTICS AND ASTRONAUTICS

at the

MASSACHUSETTS INSTITUTE OF TECHNOLOGY

February, 1965

CORRELATION OF INTERPLANETARY GEOMETRY WITH PROPULSION

REQUIREMENTS FOR OPTIMAL LOW-THRUST MISSIONS

by Neal A. Carlson

Submitted to the Department of Aeronautics and Astronautics on 29 January 1965 in partial fulfillment of the requirements for the degree of Engineer of Aeronautics and Astronautics.

ABSTRACT

The thesis develops a simple technique for preliminary mission planning based on the time-dependent orbital geometry of the launch and target planets. Numerical data is presented showing the variation with launch date and flight time of propellant requirements for ballistic and low-thrust heliocentric trajectories. The propellant requirements of each trajectory are then reduced to a characteristic length essentially independent of the propulsion mode, as observed by Zola, by application of relations derived for transfers in field-free space. The characteristic length is further shown to be a unique parameter of each trajectory which is roughly equal to the planetary separation distance near the mid-point of the transfer.

An averaged trajectory is thus defined for each actual interplanetary trajectory: that transfer in field-free space between the positions of launch and target planets at a mean trajectory time near the mid-point of the flight. The averaged trajectory model is shown to be suitable for preliminary mission planning because of the ease with which actual characteristic lengths and optimal launch dates may be approximated, and trade-offs between mission design parameters subsequently evaluated by application of field-free space relations. Machine computation of accurate trajectory data may then be localized within a neighborhood of the simply derived optimum, resulting in substantial savings of time and cost for low-thrust mission analysis.

Author

Thesis Supervisor: Walter M. Hollister, Sc. D.

Assistant Professor of
Aeronautics and Astronautics

ACKNOWLEDGMENTS

The author wishes to thank his thesis supervisor, Prof. Walter M. Hollister, for the helpful suggestions, stimulating questions, and continued encouragement that he offered throughout the progress of this study. In addition, his patience during numerous delays encountered in the investigation is greatly appreciated.

Thanks are also due LCDR Edgar D. Mitchell, who gave very generously of his time to explain the optimal control theory and trajectory optimization techniques incorporated in the digital computer program used for the numerical studies of the thesis.

The author wishes further to express his appreciation to Mrs. Ronald W. King for the long hours and conscientious effort which she devoted to typing the final draft of the thesis.

Acknowledgment is due the M.I.T. Computation Center for use of the IBM 7094 Computer. The numerical studies were performed as problem M3535.

ACKNOWLEDGMENT

CONTINUED

The printing of this publication was done under the auspices of DSR Project 5007 through National Aeronautics and Space Administration grant NsG 254-62.

The publication of this report does not constitute approval by the Experimental Astronomy Laboratory or the National Aeronautics and Space Administration of the findings or the conclusions contained herein. It is published only for the exchange and stimulation of ideas.

TABLE OF CONTENTS

TABLE OF CONTENTS (Cont.)

TABLE OF CONTENTS (Cont.)

LIST OF ILLUSTRATIONS

LIST OF ILLUSTRATIONS (Cont.)

LIST OF SYMBOLS

a	thrust acceleration
c	exhaust velocity
D	mission difficulty factor defined by eq. (5-6)
e	orbital eccentricity
F	function defined by eq. (B-9)
f	thrust
g	standard acceleration of earth gravity, 9.81 m/sec^2
I_{sp}	specific impulse
J	acceleration-squared integral defined by eq. (1-1)
k	ratio of mean trajectory time to flight time
L, L_c	characteristic length
L_g	geometric planetary separation distance
M	functional defined by eq. (B-8)
m	mass
m	mass normalized with respect to initial mass
n	mean angular motion of planet
P	power
p	power normalized with respect to initial mass
r	radial distance from the sun
T	date
t	running trajectory time measured from launch
V, v	velocity

ΔV	ideal velocity increment defined by eq. (1-2)
x	rectilinear position
α	specific mass of power plant m_s/P
β	powerplant mass fraction m_s/m_o
Δ	increment of a quantity
δ	variation of a quantity
η	engine efficiency of power conversion, P/P_s
λ	constant multiplier
$\overline{\omega}$	average of mean angular motions of launch and target planets
$\mathfrak{z}$	optimal exhaust velocity parameter defined by eq. (5-5)

Subscripts

A	arrival date
c	coast period
e	rocket engine
f	final value
L	launch date; payload
o	initial value
p	propellant
s	powerplant
1	end of acceleration period
2	start of deceleration period

Superscripts

o	optimum or minimum value
*	mean trajectory time

CHAPTER I

INTRODUCTION

Since the very beginnings of history, man's natural curiosity and spirit of adventure have led him to explore his environment. Limited only by his technological capabilities, he has ranged successively farther from his natural habitat -- over land, across the sea, and through the air. Today, technology has progressed to the extent that he stands on the brink of the last great unexplored realm of his environment, space. In addition, he stands on the verge of discovering the answer to an age-old question of philosopher and scientist alike: does life as we know it exist on other planets, or is Earth a sanctuary unique in the universe?

As the concept of space exploration has transformed from dream to reality, man has begun to plan in detail his steps through the heavens. The first step, a manned expedition to the moon, is scheduled for completion within

the decade. The second step, a manned mission to Mars, awaits advancements in propulsion technology, but nevertheless is undergoing intensive preliminary study by theoreticians.

Mission analysis is greatly complicated by the vast number of interrelated design parameters that must be considered and often compromised: scientific objective, spacecraft design, propulsion requirements, cost, reliability -- to name but a few. The first and perhaps the most important phase of mission planning seems to be the determination of propulsion requirements by optimal trajectory analysis. (Nearly all mission trade-offs or design compromises involve propellant considerations.) However, the mathematical intractability of the equations of celestial mechanics and optimization theory obscures the relationship between low-thrust propulsion requirements and optimum missions. Though the orbital motion of the planets is an easily visualized and understood phenomenon, calculation of the best way and the best time to travel from one planet to another has remained a time-consuming, tedious, and costly process. It is toward easing this situation that the present work is directed.

1.1 Power-Limited Propulsion Systems

Many interplanetary missions of scientific interest involve energy requirements well beyond the capabilities of present-day chemical rockets. The specific energy content of chemical fuels, directly related to the maximum exhaust velocity or specific impulse of the rocket, is too low to accomplish these missions without prohibitive fuel consumption.

Attention has consequently been focussed upon advanced propulsion systems capable to producing very high specific impulses. MHD and ion rockets, for example, appear capable of generating specific impulses of 1000 to 60,000 sec.[1], compared to a theoretical maximum not much over 500 sec. for chemical rockets. These high specific impulses yield very attractive mass ratios for interplanetary missions; however, this advantage is counterbalanced by the need for a separate power source to supply energy to the thrusting device. This power source and its associated equipment comprise a large percentage of the total spacecraft weight, and greatly reduce the useful payload. In addition, the power output is necessarily limited, and therefore limits the kinetic power attainable in the rocket exhaust, which in turn restricts thrust acceleration to very low levels.

The specific power output expected of power supplies within the next decade is about 0.25 kw/kg; eventual improvement by a factor of 10 may be possible[1]. The resulting thrust accelerations corresponding to the high specific impulses cited are in the range of 10^{-3} to 10^{-6} g's. Consequently, interplanetary missions will require continuous thrusting over large portions of the trajectories. Much of the difficulty inherent in mission analysis for low-thrust propulsion systems derives from this fact; the equations governing spacecraft motion cannot in general be integrated analytically when continuous-thrusting terms are involved.

The advantages and disadvantages of advanced propulsion systems are such that low-thrust rockets yield superior payloads for some missions, high-thrust rockets for others. A combination appears to be the best solution in cases where the two are closely competitive[2]. Comparative studies must be carried out to determine the most desirable system for a given mission.

The propellant requirements of power-limited propulsion systems are derived in Appendix A. In general, the

propellant consumption of a system producing constant exhaust power is directly related to the integral

$$J = \int_0^{t_f} \frac{a^2}{2} dt \tag{1-1}$$

where t_f is the flight time and a the magnitude of the thrust acceleration. Minimum propellant consumption corresponds to minimum J, and vice versa. The propellant-optimal thrust program for a particular mission is that one which minimizes J, subject to any specific constraints on thrust magnitude, and which simultaneously satisfies trajectory boundary conditions (e.g., position and velocity). An alternate measure of propellant requirements for power-limited systems producing constant (or zero) thrust magnitude -- and, in general, for any system generating constant exhaust velocity -- is the familiar ideal velocity increment

$$\Delta V = \int_0^{t_f} |a| dt \tag{1-2}$$

Minimum propellant consumption corresponds to minimum ΔV.

The separate power supply associated with advanced propulsion systems comprises, as previously noted, a

major portion of the total spacecraft weight. Since the propellant required for a given mission decreases with increasing power level, but powerplant mass at the same time increases almost linearly with power level, the powerplant can be sized to yield the maximum useful payload ratio for a given mission. As a fraction of initial spacecraft mass m_o, the optimum powerplant mass m_s is

$$\left(\frac{m_s}{m_o}\right)_{opt} = \sqrt{\alpha J} - \alpha J \qquad (1\text{-}3)$$

The resulting maximum payload ratio is

$$\left(\frac{m_L}{m_o}\right)_{max} = \left(1 - \sqrt{\alpha J}\right)^2 \qquad (1\text{-}4)$$

where the payload mass m_L is considered to include spacecraft structure. α is the ratio of powerplant mass to exhaust power, and is assumed to be independent of powerplant size. Equations (1-3) and (1-4) are derived in Appendix A.

1.2 Optimization Techniques

The determination of optimal thrust programs to minimize propellant consumption of space vehicles according to eq. (1-1) or (1-2) is a problem in the calculus of variations[3]. Classical theory has been successfully applied to the formulation of differential equations governing propellant-optimal trajectories; however, analytical solutions are generally possible only when simplifying assumptions can be made to linearize equations of motion[4,5] or to average changes in orbital parameters[6]. Exact solutions for interplanetary trajectories require numerical computation by digital computer.

Because the determination of propellant-optimal trajectories requires solution of a two-point boundary value problem, numerical computation has been a time-consuming trial-and-error procedure. Furthermore, difficulties inherent in the classical theory arise in the treatment of bounded control problems (low-thrust propulsion systems producing constant or limited exhaust velocities fall in this category), and in the development of sufficiency conditions, as opposed to necessary conditions, for optimal trajectories.

Contributions to the theory of bounded control and the existence of sufficiency conditions have been made recently by several analysts, notably Pontryagin[7], Kalman[8], and Breakwell[9]. Techniques for applying these and other optimal-control theories to machine computation have also been developed. Significant among these are Bryson's method of steepest ascent[10], Kelley's method of gradients[11], Bellman's method of dynamic programming[12], and a formulation of the method of adjoints by Mitchell[13]. These techniques all require iterative solution to the two-point boundary value problem characteristic of interplanetary trajectories, and convergence can be very slow, particularly for the interesting case of bounded control.

Despite continued computational difficulties, numerical studies of interplanetary trajectories nevertheless have met with much success. Upper and lower performance bounds for practical power-limited propulsion systems have been determined by consideration of two hypothetical propulsion systems: (1) the variable-specific-impulse (VSI) system capable of an unrestricted range of specific impulse, and (2) the constant-specific-impulse (CSI) system capable only of a fixed level of specific impulse or of coasting.

VSI trajectories are characterized by a variation in specific impulse of 100-fold or more[13]; CSI trajectories (more indicative of practical performance capabilities) are characterized by an optimal coast period occurring between two thrusting periods (the "bang-bang" or "power-coast-power" solution).

Melbourne[1] and Melbourne and Sauer[14] have applied the variational calculus to two-and-three dimensional models of the solar system to generate VSI and CSI trajectory data and propulsion requirements for both "orbiter" and "fly-by" missions to several of the planetary orbits. Application of appropriate transversality relations for unspecified terminal conditions has resulted in the determination of optimal heliocentric transfer angles and intercept positions along the target orbits for missions of fixed flight time. The existence of a propellant-optimal specific impulse and an all-propulsion lower thrust limit for CSI missions of fixed flight time is noted. In addition, it is observed that the variation of the J integral and optimal coast time with total flight time is similar to that derived analytically for optimal transfers in field-free space.

Similar investigations have been conducted by Zola[15] for CSI orbiter and round-trip missions between circular orbits representing those of Earth and Mars. His results show the effects of different thrust and power levels on fuel requirements for missions of fixed flight time. In general, higher power levels yield lower fuel consumption, and for each power level there is an optimum thrust level and an all-propulsion lower limit. As is the case with Melbourne's and Sauer's data, most of Zola's results correspond to optimized heliocentric transfer angles as well as to optimized thrust programs. Thus, heliocentric travel angle is not an independent parameter, but is chosen to have its optimum value for any given flight time.

In general, numerical studies of the type described are of particular value for the general conclusions that can be drawn regarding low-thrust payload capabilities and optimal trajectory characteristics. Generation of data even for these preliminary studies is a very costly and time-consuming process.

1.3 Mission Planning

The planning of an interplanetary mission, as previously observed, is an undertaking highly complicated by the great number of interrelated variables and design parameters to be considered. It is generally assumed that scientific objectives of the mission have been specified; mission planning in the broad sense then consists of determining the best way in which to accomplish those objectives on the basis of cost, reliability, and scientific and political exigency. Each of these criteria can be related through payload capability to necessary advancements in state-of-the-art systems technology, launch date, and mission duration. The preliminary phase of mission planning consequently can be reduced to choosing the combination of propulsion system, launch date, and flight time that maximizes the payload subject to the aforementioned constraints. (It is assumed that the propellant-optimal trajectory for any given propulsion system, launch date, and flight time will be employed.) Compromises will necessarily be made on the basis of studies quantitatively relating payload to propulsion parameters, launch date, and flight time.

For interplanetary missions taking place within the next decade, preliminary mission planning is relatively straightforward. The choice of propulsion system is limited to the chemical rocket, and payload ratios will depend primarily on the launch date and flight time. Hyperbolic excess velocities for one-way ballistic trajectories to Venus and Mars have been tabulated as functions of launch date and arrival date[16]. From these, ideal velocity increments and corresponding payload ratios can easily be calculated. Round-trip missions are similarly analyzed by pairing of outbound and inbound trajectories. The possibility of significant fuel savings by use of bi-elliptical transfers and atmospheric braking as well as by transfers via Venus (for missions to Mars) have been investigated by Hollister[17]. Velocity requirements for certain of these maneuvers are currently being tabulated[18]. For others, data is not presently available and must be generated by digital computation. However, machine computation of ballistic trajectory data is relatively fast compared to that of low-thrust data. In addition, a simple planetary model developed by Hollister can be used to predict optimal launch and arrival dates. Machine computation is then necessary only in the neighborhood of the predicted points.

Low-thrust propulsion systems will in all probability be available for interplanetary missions taking place somewhat later in the century. Studies such as those previously described indicate that, for many missions, advanced systems have considerably higher payload capability than do chemical rockets. The mission planner must then compare payload capabilities of both high- and low-thrust propulsion modes to ascertain the superior system for his particular mission. The capabilities of high-thrust propulsion are determined according to the procedure just outlined. The determination of low-thrust payload capabilities, however, is at present a far more time-consuming process. The search for optimal launch dates, flight times, and thrust levels entails the generation of a great number of trajectories and is highly costly of computer time.

The application of previous work to this search is of limited value, since results often do not take into consideration the actual time-dependent positions of the planets in their orbits. For example, the optimal heliocentric transfer angle for a 200-day flight from Earth to Mars describes relative positions of the planets that in actuality occur only once every two years (approximately).

Further specification of the optimal intercept point on the Martian orbit restricts Earth and Mars to absolute positions that may occur at the specified 200-day interval only once in scores or even hundreds of years. It is the opinion of this author that a more realistic approach for purposes of mission planning is to generate trajectory data that is related to actual planetary positions.

To reduce the computation time presently required for generating low-thrust trajectory data in the search for optimum mission parameters, Zola[15] suggests a method by which approximate low-thrust propulsion requirements can be quickly calculated. The method is based on the correlation of various modes of rocket operation by means of simple dynamical relations developed for transfers in field-free space. Zola finds that a characteristic length defined in field-free space as

$$L = \int_0^{t_f} v \, dt \tag{1-5}$$

is a very useful "linking parameter" for interplanetary trajectories. When evaluated from actual propulsion requirements by application of field-free space relations, the characteristic length turns out to be "a near-invariant

factor within and among high- and low-thrust modes of operation." Consequently, when a reference solution to a given trajectory is known, propulsion requirements for other modes of operation can be determined approximately by applying the appropriate field-free space relations to the reference characteristic length. The search for optimal trajectory parameters can be restricted to the neighborhood indicated by the correlation method, thereby greatly reducing the numerical computation required. Zola suggests ballistic trajectories as a readily available source of reference solutions, and VSI trajectories as a potential source (being more easily obtained than CSI solutions). An effective speed advantage of 100 to 1 over mission analysis by variational trajectory methods has been achieved. It is also noted in passing that the ideal velocity increment ΔV , commonly used as a measure of high-thrust propulsion requirements, is a highly variant parameter within and among the various propulsion modes.

1.4 Thesis Objectives

The existence of a characteristic length for a given interplanetary trajectory indicates a possible correlation between the planetary positions and the propulsion requirements related to a particular mission. The purpose of this thesis is to determine that correlation, and thereby to develop a simple technique for low-thrust mission planning based on the time-dependent interplanetary geometry.

CHAPTER II

RESULTS OF TRAJECTORY STUDIES

2.1 Description of the Mission and Propulsion System

Low-thrust trajectory data has been generated numerically for the heliocentric portions of three-dimensional orbiter missions between Earth and Mars. The heliocentric trajectories are assumed to start and end at the spheres of influence of the respective planets, and to be influenced only by the gravitational field of the sun. At the start of each trajectory, the spacecraft is considered just to have escaped the gravitational field of the departure planet, and therefore to possess that planet's heliocentric velocity. At the end, the spacecraft is required to match the heliocentric velocity of the target planet at its sphere of influence.

This terminal velocity constraint is the distinguishing characteristic of the orbiter mission. To be captured in a

low orbit about the target planet, the spacecraft must be decelerated within the planetary gravitational field, i.e., after entering the so-called sphere of influence. Accomplishment of this maneuver by low-thrust propulsion requires that the spacecraft have little or no velocity relative to the planet at the sphere of influence. In contrast, fly-by missions (not analyzed in this thesis) require no deceleration within the gravitational field of the target planet. Hyperbolic excess velocity is consequently of no concern, and the terminal velocity constraint on the heliocentric trajectory disappears.

The orbiter mission is assumed to take place sometime near the 1971 opposition of Earth and Mars. To determine the effects of launch date and flight time on propulsion requirements, actual three-dimensional heliocentric positions and velocities of the planets have been used as trajectory end conditions. (These quantities have been tabulated as functions of Julian date[16, 18].) The launch date fixes the initial conditions, and the flight time fixes the arrival date and the corresponding final conditions.

Trajectory data has been generated for both VSI and CSI propulsion modes by use of the computational technique developed by Mitchell and Krupp[13]. Convergence is very quick for VSI trajectories, but generally unsatisfactory for CSI trajectories. Consequently CSI data is limited. All numerical results correspond to the same ratio of exhaust power to initial spacecraft mass, since the optimization of launch date and flight time, independent of power variation, is the objective of these studies. The power ratio chosen,

$$\frac{P}{m_o} = 0.0242 \ \frac{kw}{kg}$$

corresponds to a conservative value of powerplant specific mass,

$$\alpha = \frac{m_s}{P} = 10 \ \frac{kg}{kw}$$

and to a powerplant mass fraction of

$$\frac{m_s}{m_o} = 0.242$$

which has been chosen from eq. (1-3) to maximize the payload ratio when J=0.017 m^2/sec^3. (This value of J is within the range obtained for 150- to 200-day VSI trajectories.)

The effects of different power levels have been previously analyzed. In general, the J integral is relatively independent of power ratio except for very low power levels[1]; higher final-to-initial mass ratios then result from higher power levels, and vice versa[15]. This relationship is evident from eq. (2-2).

2.2 Low-Thrust Propulsion Requirements

The propellant requirements of numerically computed trajectories are measured for purposes of illustration by the integral

$$J = \int_0^{t_f} \frac{a^2}{2}\, dt \qquad (2\text{-}1)$$

Recall that minimum values of J correspond to minimum propellant consumption, or maximum final mass. The exact relation, from Appendix A, is

$$\frac{m_0}{m_f} = 1 + \frac{m_0}{P} J \qquad (2\text{-}2)$$

where m_f is the final mass. Launch dates are given in terms of Julian date. (Julian date increases each day by 1.0. For reference, J. D. 244 1150.0 corresponds to the calendar date July 18, 1971, at noon.) The 1971

opposition of Mars occurs at J. D. 244 1173.8, or 10.3 August. This date will henceforth be denoted by T_{opp}.

Figures 1-4 show the variation of J with launch date (T_L) and flight time (t_f) for propellant-optimal VSI trajectories. (For purposes of clarity, the upper-case T is used to indicate date, the lower-case t to indicate trajectory time measured from launch. Thus t = 0 when $T = T_L$, $t = t_f$ at the arrival date T_A, and $T = T_L + t$ in general.)

Note the similarity between the propellant requirements for Earth-to-Mars (E-M) trajectories shown in Figure 1 and those for Mars-to-Earth (M-E) trajectories shown in Figure 2. The propellant-optimal launch date (T_L^*) for each flight time occurs approximately half the flight time prior to opposition, the exact difference, $T_{opp} - T_L^*$, being somewhat less than $\frac{1}{2} t_f$ for E-M transfers and about the same amount greater than $\frac{1}{2} t_f$ for M-E transfers. This relationship is clarified in Figure 3, where each curve has been shifted forward in date by one-half the appropriate flight time. The nearly identical minimum values and shapes of each pair of curves are also apparent.

Figure 4 shows the effect of non-coplanarity on propulsion requirements for 150-day VSI trajectories from Earth to Mars. For the coplanar trajectories, position and velocity components of Mars out of the earth's ecliptic plane are set equal to zero. The coplanar components are then used as trajectory terminal conditions. The one to two percent increase in J between corresponding coplanar and non-coplanar trajectories illustrates the small effect of the orbital inclination of Mars on VSI propulsion requirements. This small effect has been observed previously[14] and attributed both to the small inclination involved, 1.85°, and to the relative plane-changing efficiency of continuous thrusting. The high propellant penalties characteristic of ballistic transfers between non-coplanar orbits for which the heliocentric transfer angle approaches 180° are not observed for corresponding low-thrust trajectories. Particular examples from Figure 2 are the 180-day and 210-day E-M trajectories launched near J. D. 244 1170.5 and J. D. 244 1100.5, respectively.

Comparison of corresponding VSI and CSI propellant requirements for 180-day E-M trajectories are shown in

Figure 5. As predicted and observed by other analysts[1, 13], CSI propulsion results in somewhat higher values of J than does the VSI mode. The specific impulse chosen for the CSI trajectories, 3210 sec, is intermediate among the initial values observed for the corresponding VSI trajectories. The related initial thrust acceleration is 1.573 x 10^{-4} g's. Of particular interest here is the fact that the optimal launch date is the same for both propulsion modes. Similar data for other flight times and specific impulses has not been generated because of the poor convergence of the computational technique for CSI trajectories.

Figure 6 illustrates the variation of J with specific impulse for two CSI missions of fixed launch date and flight time. For comparison, points representing the J value and initial specific impulse from the corresponding VSI missions have been encircled. Note that the optimal specific impulse is somewhat greater than the initial value of the VSI propulsion mode, and somewhat less than the all-propulsion upper limit. The upper limit corresponds to the minimum value of thrust with which the mission may be accomplished by CSI propulsion. The existence for a particular mission of an optimal CSI

specific impulse somewhat greater than the initial VSI value is predicted by the relations for transfers in field-free space derived in Appendix B.

The variation of propulsion requirements with flight time is often of interest to the mission planner. Figures 1 and 2 indicate that for VSI trajectories starting from optimal launch dates, longer flight times in general result in lower propellant requirements. This result is also apparent from more extensive data generated by Melbourne[1] for missions of optimal heliocentric transfer angle. The variation of propellant requirements with flight time for missions starting from a fixed launch date, however, have not to the author's knowledge been analyzed. The effect of changing the arrival date and hence the flight time is of particular importance after a spacecraft already has been launched on an interplanetary mission. Knowledge of the variation of propellant requirements with remaining flight time is then applicable to changes in flight plan (perhaps to counteract unforeseen circumstances) as well as to variable-time-of-arrival guidance analysis[13].

Figure 7 shows the variation of J with flight time for both CSI and VSI missions starting from a fixed launch date. Data is incomplete due to thesis time limitations, yet certain trends are apparent. For short flight times of 200 days or less, increasing the flight time reduces propulsion requirements of both VSI and CSI trajectories. For longer flight times, further propellant reduction is minimal. In fact, there may exist an optimal flight time at which the required propellant reaches at least a relative minimum. The dashed curves, representing propellant predictions based on the method developed in Chapter V, exhibit minimum values. However, the generation of further numerical data to confirm or refute these predictions is necessary.

It should be noted in passing that the phenomenon of infinite switching (switching between power-on and power-off operation at infinitesimal time intervals) has been observed for CSI missions employing thrust levels greater by factors of only two or three than the optimal values for those missions. Infinite switching is a mathematical singularity not easily interpreted in physical terms. It is undoubtedly related to the situation

in which a so-called "switching function" remains constant at the switching value over a finite time interval. The switching function is a continuous variable derived by the application of optimal control theory to the minimization of propellant consumption for CSI trajectories[13]. It effectively tells the propulsion system when to thrust and when to coast. When it is greater than a certain value, the optimal operation is maximum thrust; when less, the optimal operation is minimum thrust (zero). In most cases, the switching function is equal to the switching value only instantaneously. However, should it remain at the switching value over a finite time interval, the optimal thrust magnitude is indeterminate by the present theory for trajectories in an inverse-square central force field[3]. The observed infinite-switching phenomenon may indicate that the optimal thrust magnitude in that region is intermediate between maximum and minimum. Furthermore, since the theory does not restrict operation to only one coast period (the "power-coast-power" solution), it also appears that for certain missions the propellant-optimal CSI trajectories may in fact require more than one coast period. Further research in this area is recommended.

For comparison with the propulsion requirements of low-thrust missions, Figures 8 and 9 show the total ΔV required for ballistic trajectories between Earth and Mars. ΔV is the sum of the hyperbolic excess velocities at the two planets, and effectively measures the propellant required to transfer between the planetary spheres of influence. The similarity between corresponding curves for E-M and M-E trajectories is again apparent. Note also that $T_{opp} - T_L$ is again somewhat less than $\frac{1}{2}\ t_f$ for E-M transfers and about the same amount greater than $\frac{1}{2}\ t_f$ for M-E transfers, at least for the shorter flight times. The drastic propellant increases in the neighborhood of certain launch dates for the 180- and 210-day trajectories correspond to the heliocentric transfer angle's approaching 180°. Thus the effect of non-coplanarity is very serious for two-impulse ballistic trajectories. The dashed curves represent broken-plane trajectories, in which a third relatively small impulse near mid-trajectory accomplishes the necessary plane change. The propellant requirements are thereby significantly reduced for near-180° transfers. It is apparent that the correlation of ballistic and low-thrust propulsion requirements as suggested by Zola will be valid only when heliocentric transfer angles are not close to 180° or when two-dimensional (coplanar) ballistic solutions are employed.

CHAPTER III

CHARACTERISTIC LENGTHS

The concept of a characteristic length with which to correlate propellant requirements of a given mission within and among the various modes of rocket operation has been suggested by Zola. The characteristic length is defined for rectilinear transfers in field-free space (FFS) as

$$L = \int_0^{t_f} v \, dt \tag{3-1}$$

and is, quite simply, the distance travelled within the specified flight time t_f. The propellant requirements for impulsive (ballistic), VSI, and CSI point-to-point transfers in FFS are derived in Appendix B. The constraint that initial and final velocities be zero is applied, analogous to the boundary conditions on velocity for interplanetary orbiter trajectories. The relations for

propellant requirements can be inverted to yield explicit expressions for L:

(Impulsive) $$L = \frac{1}{2} \Delta V \, t_f \tag{3-2}$$

(VSI) $$L = \sqrt{\frac{J t_f^3}{6}} \tag{3-3}$$

(CSI) $$L = -c t_f \ln m_1 + \frac{c^3}{2p}\left[(1-m_1)^2 + (1-m_1^2)\ln m_1\right] \tag{3-4}$$

where m_1 and p are defined for convenience as

$$m_1 = \sqrt{\frac{m_f}{m_o}} \tag{3-5}$$

$$p = \frac{P}{m_o} \tag{3-6}$$

and c is the exhaust velocity. The ideal velocity increment

$$\Delta V = \int_o^{t_f} |a| \, dt \tag{3-7}$$

is also derived in Appendix B for FFS transfers. For the various propulsion modes it is

{Impulsive and CSI} $$\Delta V = -2c \ln m_1 = -c \ln (m_f/m_o) \tag{3-8}$$

(VSI) $$\Delta V = \sqrt{\frac{3}{2} J t_f} \tag{3-9}$$

Characteristic length for actual interplanetary trajectories are calculated by substitution of the numerically-computed values of J or m_1 into the appropriate expression (3-2), (3-3), or (3-4). Ideal velocity increments are similarly calculated from (3-8) or (3-9). The actual values of t_f, c, and p must of course be used. As discussed in Chapter II, all numerical trajectory data corresponds to the power ratio p=0.0242 kw/kg.

3.1 Correlation by Characteristic Length

Figure 10 shows the characteristic lengths (L_c) of 180-day Earth-to-Mars trajectories calculated over a range of launch dates for each propulsion mode. The close agreement among the curves verifies the relative independence of characteristic length upon propulsion mode. In contrast, Figure 11 illustrates the poor correlation achieved for the same trajectories by use of the ideal velocity increment ΔV.

Figure 12 shows the characteristic length and the ideal velocity increment calculated over a range of exhaust velocities for two CSI missions of fixed launch date and flight time. The near-invariance of characteristic

length within the CSI mode of operation is evident; again, ΔV is a highly-variant parameter with which poor correlation is achieved.

No data is presented to verify the invariance of characteristic length within the VSI or impulsive modes. Within the VSI mode, the only propulsion parameter which can be chosen arbitrarily is the power ratio p. It can be shown analytically that the propellant-optimal acceleration program for a VSI trajectory is independent of p; consequently neither J nor the characteristic length derived therefrom can vary within the VSI mode for a particular mission.

In the case of impulsive thrusting, only one (practical) two-impulse ballistic trajectory exists for a particular mission. Tne hyperbolic excess velocities at the planetary spheres of influence are thereby fixed. The sum of their magnitudes is the ΔV required for the heliocentric transfer, independent of thrust level or specific impulse. Consequently the characteristic length, dependent only upon ΔV and t_f from eq. (3-2), must be invariant within the impulsive mode for a particular mission.

3.2 Characteristic Lengths from Trajectory Studies

The characteristic lengths of VSI and ballistic trajectories between Earth and Mars are shown as functions of launch date and flight time in Figures 13 through 16. The values have been calculated from the corresponding propellant requirements illustrated in Figures 1, 2, 8, and 9. Note that since characteristic length varies directly with J (VSI) or ΔV (impulsive), it is itself a direct measure of the propellant required for a particular trajectory. Thus the optimal launch date $T_L^{\bullet}$ for a given flight time corresponds to the minimum value of L_c. As observed in Section 2.2, the optimal launch date for each flight time occurs approximately half the flight time prior to the date of planetary opposition, T_{opp}. The exact difference in date, $T_{opp} - T_L^{\bullet}$, is somewhat less than $\frac{1}{2}t_f$ for E-M trajectories, and about the same amount greater than $\frac{1}{2}\ t_f$ for M-E trajectories. The discrepancy between $T_{opp} - T_L^{\bullet}$ and $\frac{1}{2}\ t_f$, particularly evident in Figure 3, seems to increase in rough proportion with t_f.

Perhaps the most interesting feature of the characteristic length curves is that the minimum values are nearly identical for E-M and M-E trajectories of the same flight

time; further, they vary only slightly with flight time itself, decreasing gradually as flight time increases. In fact, not only the minimum values but the entire curves are remarkably similar among the various flight times. (The only exceptions to these general observations occur for the previously mentioned ballistic trajectories of near-180 heliocentric transfer angle.)

3.3 Interplanetary Geometry

It is instructive at this point, keeping in mind the variation of characteristic length with launch date, to examine the time-dependent positions of Earth and Mars in their respective orbits. In particular, consider the line-of-sight or "communication" distance between the two planets. Figure 17 shows this geometric length (L_g) as a function of Julian date near opposition. The variation of L_g with date is caused by the earth's possessing a greater angular velocity about the sun than does Mars; the earth catches up to Mars and "passes" it at opposition. The minimum geometric length occurs slightly after opposition because Mars is approaching its aphelion point, and the two orbits are nearing their minimum radial separation (not to be confused with planetary separation).

By comparison of Figures 17 and 13-16, it is apparent that the variation of L_g with Julian date near opposition bears marked resemblance to the variation of characteristic length near the optimal launch dates. The generally parabolic curve-shapes are quite similar, and the minimum values are roughly the same (within 10 to 15%). In fact, were the planetary separation shown in Figure 17 superposed on the characteristic length diagrams at the appropriate dates, it would be consistent with the observed trends of optimal launch dates and decreasing minimum values.

A little thought should indicate that the geometric planetary separation at a particular date <u>is</u>, in actuality, the characteristic length for the VSI or impulsive trajectory departing from either planet on that date and arriving after an infinitesimal flight time at the other planet, effectively on the same date. In other words,

$$L_g = \lim_{t_f \to 0} L_c \qquad (3\text{-}10)$$

For small flight times, the spacecraft accelerations and velocities are much greater, respectively, than the gravitational acceleration due to the sun or the heliocentric velocities of the planets. In the limit, as t_f approaches zero, the latter are completely negligible, and

the interplanetary trajectory becomes essentially a point-to-point transfer in FFS. The distance travelled in FFS (here, the planetary separation distance) is by definition the characteristic length.

It has previously been observed that orbital eccentricity can be of significant effect on interplanetary propulsion requirements, but that orbital inclination is of very little. The explanation is very simple in terms of planetary separation and characteristic length. The relatively large eccentricity of the Martian orbit (e=0.093) causes its radial distance from the earth's slightly-elliptic orbit (e=0.017) to vary from 0.37 a.u. at perihelion to 0.68 a.u. at aphelion. Consequently, the planetary separation L_g for "favorable" oppositions occurring near the Martian perihelion point will be closer to 0.37 a.u.; the separation for "unfavorable" oppositions occurring near the aphelion point will be closer to 0.68 a.u. Assuming that a correlation exists between characteristic length and geometric planetary separation, one would then expect the optimum characteristic lengths to vary much in the same proportion (1.84:1) between favorable and unfavorable oppositions. The corresponding J integrals

would then vary according to the square, or by a factor of approximately 3.4. Melbourne and Sauer's data[14] shows an analogous variation by a factor of 3.5 for trajectories corresponding to optimal transfer angles and different intercept points on the Martian orbit.

The orbital inclination of Mars (1.85°) causes Mars to reach its maximum distance below the earth's ecliptic plane (0.045 a.u.) near the 1971 opposition. The minimum planetary separation is then 0.375 a.u., about 0.7% larger than its projection on the ecliptic. Thus, going from coplanar to non-coplanar trajectories should increase values of L_c by about 0.7%, and of J by about 1.4%. Numerical data shown in Figure 5 shows an actual increase of roughly 2%.

Opposition periods of Mars occur approximately at 780-day intervals. The next few favorable oppositions will occur in 1971, 1986, and 1988; unfavorable oppositions will occur in 1965, 1978, and 1980.

Conjunctions of Earth and Venus occur very nearly at 580-day intervals, the next in early 1966. The orbit of Venus is very nearly circular (e=0.007), and is inclined

$3.40^{\bullet}$ from the ecliptic plane. The radial separation between the orbits varies only from 0.265 to 0.289 a.u.; hence, values of J should vary by less than 20% between favorable and unfavorable conjunctions. The effect of orbital inclination on J should again be small, about 1%. Favorable conjunctions occur in 1966, 1974, and 1982; unfavorable, in 1967, 1972, 1975, 1980, and 1983. The differences are relatively small for propulsion purposes.

CHAPTER IV

CORRELATION OF CHARACTERISTIC LENGTH WITH INTERPLANETARY GEOMETRY

4.1 Functional Relationships of Characteristic Length

The basic functional dependence of characteristic length on the various mission parameters has been investigated in Chapter III and can now be summarized. Characteristic length is nearly independent of the mode of rocket operation, and of the power and thrust levels within a particular mode. It is, however, strongly dependent upon launch date and flight time, and hence to the associated interplanetary geometry. For a fixed flight time, the magnitude and variation of characteristic length near the optimal launch date are very similar to the magnitude and variation of planetary separation distance near the subsequent opposition date. The optimal launch date occurs approximately half the corresponding flight time prior to opposition; the associated minimum

value of characteristic length is only weakly dependent upon t_f, gradually decreasing with longer flight times.

4.2 Mean Trajectory Time

The characteristic length and the interplanetary geometry associated with a particular mission can be closely correlated by a parameter t* which shall be designated the "mean trajectory time." Consider the following argument. Characteristic length is a direct measure of the total propellant consumption and hence of the average propulsion requirements associated with a particular mission. Minimum characteristic length (for a given flight time) results when the minimum separation of launch and target planets occurs at approximately half the total flight time after launch, and is roughly equal to that geometric distance. In fact, the rough equality also holds true for non-minimum characteristic lengths and planetary separations -- as long as the pertinent planetary separation is chosen to be that at approximately half the flight time after launch. Thus the characteristic length is correlated with planetary separation, not at the beginning or end of a trajectory, but at a particular time along the trajectory which is

near half the total flight time. This particular time is defined as the "mean trajectory time," t*. Note that t* is not directly related to date except through the launch date for a given trajectory. It is simply the particular instant in running trajectory time, measured from launch, at which the simultaneous planetary separation is best correlated with the characteristic length. Specifically, since planetary separation L_g is solely a function of date, and characteristic length L_c is a significant function only of launch date and flight time, the correlation can be summarized by the expression

$$L_c(T_L,\ t_f) \approx L_g(T_L + t^*) \tag{4-1}$$

Note that the minimum characteristic length occurs for a given flight time when $T_L + t^* = T_{opp}$. Thus the optimal launch date is

$$T_L^{\bullet}(t_f) = T_{opp} - t^*(t_f) \tag{4-2}$$

Mean trajectory time evidently is of little practical use for calculating approximate characteristic lengths from eq. (4-1) unless it can be evaluated from known mission parameters: launch date, flight time, and the

associated geometry of the planets. Examination of Figures 13, 14, and 17 reveals a very simple relationship between t* and mission parameters for VSI missions. Since the shapes of the characteristic-length curves are quite similar to that of the planetary-separation curve, t* must be nearly independent of launch date for a given flight time. The variation of t* with t_f can then be determined from the variation of T_L with t_f. Figures 13 and 14 indicate this variation to be nearly linear; hence t* is, to good approximation, linearly proportional to t_f:

$$t^* \approx k\, t_f \tag{4-3}$$

For E-M trajectories, k is somewhat less than ½; for M-E trajectories, k is about the same amount greater than ½ (see Figure 3). If the k's of the respective trajectory directions are designated as k_{em} and k_{me}, the relationship is

$$k_{em} \approx 1 - k_{me} \tag{4-4}$$

It will be noted from Figures 13 and 14 that the actual values of k_{em} and k_{me} for VSI trajectories near the 1971

opposition are about 0.45 and 0.55, respectively.

Mean trajectory times for ballistic trajectories can be approximated in the same manner. The characteristic-length curves shown in Figures 15 and 16 are not quite as similar to one another as are the corresponding VSI curves, due to the large effect of non-coplanarity on near-180° ballistic transfers. Consequently, the k of eq. (4-3) varies somewhat with launch date and flight time. However, optimal launch dates can still be determined approximately by using eqs. (4-2), (4-3), and the k for VSI trajectories.

The relationship of mean trajectory time to total flight time can be interpreted qualitatively on physical grounds. Consider the potential energies of Earth, Mars, and the spacecraft within the gravitational field of the sun. Since potential energy varies inversely with radial distance from the sun, the average potential energy of the transfer occurs at a radial distance closer to the earth's orbit than to the Martian orbit. Thus the spacecraft can be expected to achieve its average potential energy at less than half the flight time for E-M transfers, and at more than half the flight time for M-E transfers.

Furthermore, since the heliocentric angular velocity of the earth is greater than that of Mars, and the spacecraft angular velocity changes smoothly from one to the other during a transfer, the spacecraft will accomplish half its total angular travel in less than half the flight time for E-M missions, and in more than half the flight time for M-E missions. Consequently, the mean trajectory time seems to be that time at which the spacecraft arrives at the point on the trajectory most representative of the total transfer. The most representative point is that one which best averages the radial motion according to the potential energy change, and the circumferential motion according to the heliocentric angular change. Since radial and circumferential motions along actual VSI trajectories are respectively similar for different flight times (just stretched out in time, more or less, according to the total flight time available), it is reasonable to expect the mean trajectory time to be proportional to flight time. Furthermore, since these motions are effectively reversed between M-E and E-M trajectories, it is also reasonable to expect the respective mean trajectory times to be related according to eq. (4-4): one mean trajectory time is very nearly

the difference between t_f and the reverse mean trajectory time.

Mean trajectory times can be calculated approximately in the following manner. Determine the radial distances from the sun of the launch planet at T_L and the target planet at arrival. Call these r_L and r_T. The radial distance corresponding to the average potential energy is then

$$\bar{r} = \frac{2 r_L r_T}{r_L + r_T} \tag{4-5}$$

The fractional radial distance that the spacecraft must travel to achieve the average potential energy is

$$\frac{\overline{\Delta r}}{\Delta r_{tot}} = \frac{\bar{r} - r_L}{r_T - r_L} \tag{4-6}$$

The time required to travel this fractional distance is evaluated by considering the radial motion to be that of a rectilinear VSI transfer in FFS. The appropriate FFS equation relating fractional trajectory time to fractional distance travelled (derived in Appendix B) is, for the

case at hand,

$$\frac{\Delta r(t)}{\Delta r_{tot}} = 3\left(\frac{t}{t_f}\right)^2 - 2\left(\frac{t}{t_f}\right)^3 \qquad (4\text{-}7)$$

Substituting (4-6) into eq. (4-7) yields the approximate value of t=t* for the trajectory. For convenience, eq. (4-7) is shown plotted in Figure 18; the variation of Δr with time is remarkably similar to that for actual VSI trajectories. Mean trajectory times calculated in this manner agree with those observed at the optimal launch dates (Figures 13 and 14) to within a few percent. In fact, the values of k so derived vary very little; essentially the same accuracy can be attained using the fixed values

$$k_{em} \approx 0.45$$

$$k_{me} \approx 0.55$$

For interplanetary missions to the outer planets, such as to Jupiter or to Saturn, the spacecraft must undergo a much larger percentage change in orbital angular momentum than in energy. Thus the "best" average point along the trajectory may well be better determined

on the basis of angular momentum than on that of energy. Since angular momentum is roughly proportional to $r^{\frac{1}{2}}$, energy to r^{-1}, the angular momentum average will occur at a greater distance from the sun than the energy average. Outbound mean trajectory times based on averaged angular momentum would thus be greater than those based on averaged energy. No trajectory data has been generated by the author to check such cases.

CHAPTER V

THE AVERAGED TRAJECTORY IN FIELD-FREE SPACE

5.1 The Averaged Trajectory

The results of Chapters III and IV indicate that interplanetary transfers can be vastly simplified for purposes of calculating optimal launch dates and approximate propulsion requirements. The following summary will serve to elucidate those results.

Mean trajectory time effectually averages the positions of the launch and target planets with respect to the spacecraft during an interplanetary transfer. The geometrical separation distance between the averaged planetary positions is roughly equal to the characteristic length of the actual trajectory; it is identically equal to the characteristic length of the rectilinear transfer between those points in field-free space. Further, the

characteristic length is a measure of the total propellant consumption, and hence of the averaged propulsion requirements of a trajectory. It may thus be concluded that actual trajectory propulsion requirements are approximated by those of a rectilinear transfer in FFS between the positions of the launch and target planets at the mean trajectory time. This FFS transfer will be designated the "averaged trajectory".

The averaged trajectory is a simplified model of the true interplanetary trajectory. It is of particular value to mission planning because of the resulting ease with which optimal launch dates and approximate propulsion requirements can be calculated. The only data necessary for these calculations are the planetary positions as functions of date, and certain parameters describing the propulsion system: exhaust velocity (impulsive), power-to-mass ratio (VSI), or both (CSI). The simple forms of the appropriate FFS equations and propellant relations allow rapid hand calculation of desired quantities. The averaged-trajectory model is most useful in the analysis of low-thrust transfers, but may be applied as well to ballistic trajectories for which the heliocentric transfer

angles are not close to 180 deg.

5.2 Optimum Specific Impulse for CSI Trajectories

The fact that the propulsion requirements of an actual interplanetary trajectory are approximated by those of an averaged transfer in FFS suggests that further properties of low-thrust trajectories can be derived by application of FFS relations. Examples are presented in this and the next section.

First, consider the variation of propellant requirements with specific impulse, or exhaust velocity, for CSI trajectories. As noted in Section 2.2 and illustrated in Figure 6, there exists an optimum exhaust velocity for any given mission and power level. By applying appropriate FFS relations (derived in Appendix B) to the characteristic length of the given mission, the approximate optimum exhaust velocity can be readily calculated.

The characteristic length of the mission is assumed to be known. For a CSI transfer in FFS, it is related to the exhaust velocity and final mass ratio by eq. (3-4), repeated here for convenience:

$$L = -ct_f \ln m_1 + \frac{c^3}{2p}\left[(1-m_1)^2 + (1-m_1^2)\ln m_1\right] \qquad (5\text{-}1)$$

where, again,

$$m_1 = \sqrt{\frac{m_f}{m_o}} \tag{5-2}$$

and

$$p = \frac{P}{m_o} \tag{5-3}$$

The optimum exhaust velocity c_{opt} is that value which maximizes m_1 and, hence, minimizes propellant consumption. c_{opt} is evaluated by straightforward differentiation of eq. (5-1) with respect to c. The algebra is carried out in Appendix B; the result is

$$\frac{1}{D} J^3 - \left(1 - e^{-2J}\right) J + \left(1 - e^{-J}\right)^2 = 0 \tag{5-4}$$

where the optimum exhaust velocity is

$$c_{opt} = \frac{1}{J} \frac{3L}{2t_f} \tag{5-5}$$

and D is a mission "difficulty factor" defined as

$$D = \frac{27 L^2}{8 p t_f^3} \tag{5-6}$$

The resulting maximum value of m_1 is

$$(m_1)_{max} = e^{-f} \tag{5-7}$$

Note that eq. (5-4) can be solved analytically for the limiting cases of very small and very large mission difficulty factors. The following expressions are easily derived:

$D \ll 1$

$$f \approx D \tag{5-8}$$

$$c_{opt} \approx \frac{4pt_f^2}{9L} \tag{5-9}$$

$$(m_1)_{max} \approx 1 - D \tag{5-10}$$

$D \gg 1$

$$f \approx \sqrt{D} \tag{5-11}$$

$$c_{opt} \approx \sqrt{\frac{2}{3} p t_f} \tag{5-12}$$

$$(m_1)_{max} \approx e^{-\sqrt{D}} \tag{5-13}$$

It is instructive to determine the relationship between the optimal exhaust velocity for CSI transfers and the initial exhaust velocity for (propellant-optimal) VSI transfers in FFS. From Appendix B, the initial exhaust velocity c_o for the VSI transfer is

$$c_{o(VSI)} = \frac{p t_f^2}{3L} = \frac{1}{D} \frac{9L}{8 t_f} \tag{5-14}$$

Combining eqs. (5-5) and (5-14) yields

$$c_{opt} = \frac{D}{J} \frac{4}{3} c_{o(VSI)} \tag{5-15}$$

The relation $D \geq J$ is easily verified from eq. (5-4); the equality holds only in the limit as D approaches zero. Thus eq. (5-5) implies that, for all $D \geq 0$,

$$c_{opt} \geq \frac{4}{3} c_{o(VSI)} \tag{5-16}$$

This result is in agreement with the data shown in Figure 6.

The all-propulsion upper limit on the exhaust velocity for a CSI mission can also be derived. This limit corresponds to the lowest thrust level with which the mission can be accomplished; no coast period is

possible. The equation corresponding to (5-1) for the case of zero coast time is

$$L = \frac{c^3}{2p}\left(1 - \sqrt{1 - \frac{2pt_f}{c^2}}\right)^2 \tag{5-17}$$

Eq. (5-17) cannot in general be solved explicitly for the limiting exhaust velocity, c_{lim}. However, for the special cases in which $D \ll 1$ or $D \gg 1$, the limiting values can be determined:

$$(D \ll 1) \qquad c_{lim} \approx \frac{pt_f^2}{2L} \tag{5-18}$$

$$(D \gg 1) \qquad c_{lim} \approx \sqrt{2pt_f} \tag{5-19}$$

Comparison of eqs. (5-18) and (5-19) with (5-9) and (5-10), respectively, reveals that the all-propulsion upper limits are only slightly greater than the corresponding optimum values of exhaust velocity. In particular,

$$(D \ll 1) \qquad c_{opt} \approx \frac{\sqrt{8}}{3} c_{lim} \tag{5-20}$$

$$(D \gg 1) \qquad c_{opt} \approx \frac{\sqrt{3}}{3} c_{lim} \tag{5-21}$$

These results, too, agree generally with observations from numerical trajectory studies[14, 15].

A sample calculation of optimum exhaust velocity will illustrate the method. Consider the 150-day E-M mission launched at T_L=J. D. 244 1080.5. (This mission is one of the two for which numerical data is presented in Figure 6.) The mean trajectory time for the mission is

$$t^* = k_{em}\, t_f = 67.5 \text{ days}$$

where the value 0.45 has been used for k_{em}, as suggested in Section 4.2. The date corresponding to the mean trajectory time is thus

$$T^* = T_L + t^* = \text{J. D. } 244\ 1148.0$$

The planetary separation at T* is found from Figure 17 to be

$$L_g(T^*) = 0.428 \text{ a.u.}$$

This value is the characteristic length of the averaged trajectory, and is roughly (within 12%) equal to the characteristic length of the actual trajectory.

Thus

$$L_c \approx L_g = 0.428 \text{ a.u.}$$

Recall that the power ratio is

$$p = 0.0242 \frac{kw}{kg} = 0.6988 \times 10^{-6} \frac{au^2}{day^3}$$

Then the mission difficulty factor, by eq. (5-6) is

$$D = 0.262$$

To evaluate f, eq. (5-4) must be solved by trial and error. For the first trial, use a value for f somewhat less than the actual D, say f'. Then calculate the corresponding value D' from eq. (5-4). For the next trial, use the value f'' calculated from the equation

$$f'' = \left(\frac{f'}{D'}\right) D_{actual} \tag{5-22}$$

This iterative process converges very quickly. The value of f for the present case is found to be

$$f = 0.214$$

The optimum exhaust velocity is then calculated from eq. (5-5) to be

$$C_{opt} = 0.0200 \frac{au}{day} = 34,600 \frac{m}{sec}$$

(The conversion factor is 1.0 au/day=1.7315 x 10^6 m/sec.)

The corresponding optimal specific impulse is

$$(I_{sp})_{opt} = \frac{c_{opt}}{g} = 3530 \text{ sec}$$

A more accurate value for c_{opt} can be calculated by using the characteristic length of the corresponding VSI trajectory in eqs. (5-5) and (5-6). From Figure 13, this value is

$$L_c = 0.381 \text{ a.u.}$$

Carrying out the preceding calculations once more yields the following results:

$$D = 0.208$$

$$\mathcal{J} = 0.176$$

$$c_{opt} = 0.0216 \frac{au}{day} = 37,500 \frac{m}{sec}$$

$$(I_{sp})_{opt} = 3820 \text{ sec.}$$

For purposes of comparison, the true optimum exhaust velocity and specific impulse for the mission can be determined from the numerical data shown in Figure 6.

They are

$$c_{opt} = 0.0211 \frac{au}{day} = 36{,}600 \frac{m}{sec}$$

$$(I_{sp})_{opt} = 3730 \text{ sec.}$$

The approximate values calculated by the simple technique are remarkably accurate: the error is less than 6% in the first case, less than 3% in the second. A few minutes of slide-rule work have yielded essentially the same results as several trajectory runs on the digital computer -- plus a great deal more insight into the effects of the several variables involved.

5.3 Optimal Flight Time

The variation of low-thrust propellant requirements with flight time has been discussed in Section 2.2. From the results of numerical studies, it appears that propellant requirements for both VSI and CSI missions decrease monotonically as the flight times increase -- provided that the optimal launch date is chosen for each flight time. Choosing the optimal launch date for each t_f effectively picks the trajectory of minimum characteristic length for that flight time. Each of these trajectories

can thus be approximated by the same averaged trajectory in FFS: that between the positions of the launch and target planets at opposition. It is a well-known result that the propellant requirement of a fixed low-thrust transfer in FFS decreases continuously as the available flight time increases. This result is evident from the now-familiar characteristic-length equations

$$(\text{VSI}) \qquad L = \sqrt{\frac{J t_f^3}{6}} \tag{5-23}$$

$$(\text{CSI}) \qquad L = -c t_f \ln m_1 + \frac{c^3}{2p}\left[(1-m_1)^2 + (1-m_1^2)\ln m_1\right] \tag{5-24}$$

When L is fixed, increasing t_f without limit reduces J continuously to zero and increases m_1 continuously to 1.0, both of which correspond to reducing the propellant consumption to zero. This general conclusion is not altered by the fact that actual minimum values of L_c actually decrease gradually with flight time, as shown in Figures 13 and 14.

For the case in which the launch date is fixed, the above conclusion is no longer valid. Each flight time corresponds to a different averaged trajectory, and hence

to a different characteristic length. The characteristic length is roughly equal to the planetary separation distance at the mean trajectory time $t^* = kt_f$, as indicated by the relation

$$L_c\ (T_L,\ t_f) \approx L_g\ (T_L + kt_f) \tag{5-25}$$

The minimum values of L_g and L_c occur when $T_L + kt_f = T_{opp}$. Then, when $kt_f < T_{opp} - T_L$ (where T_L is fixed), a further increase in t_f will reduce L_g and L_c; however, when $kt_f > T_{opp} - T_L$, further extending the flight time will cause both to increase. For any given launch date, then, increasing t_f without bound will eventually cause the characteristic length in eqs. (5-23) and (5-24) to grow larger. If L_c should increase rapidly enough, a point will be reached at which further extension of the flight time will require greater fuel expenditure. Consequently, it is likely that for missions starting from certain launch dates there exist finite flight times at which the propellant consumption is locally minimized.

The variation of propellant requirements with flight time for missions of fixed launch date is of little

concern for preliminary mission planning. In general the optimal launch date will be chosen for any particular flight time, though in some situations the launch date may be restricted. In the more advanced stages of mission planning, however, the effects on propellant consumption of changing the mission flight plan while the spacecraft is en route must be determined. The variation of propellant requirement with flight time from a fixed launch date is particularly relevant to that analysis, and to the related study of variable-time-of-arrival guidance techniques.

The variation of propellant with flight time can be evaluated quantitatively as well as qualitatively by use of the averaged-trajectory concept and the associated FFS equations. The procedure is simply to evaluate J or m_1 for various flight times from eqs. (5-23) or (5-24), using as the characteristic lengths the approximate values calculated as functions of flight time from eq. (5-25). The dashed curves of Figure 7 show the results of sample calculations carried out in this manner for both the VSI and CSI modes of propulsion; the solid curves represent actual numerical data for the same missions. Observe that

the curves derived simply from the averaged trajectory model exhibit the same trend of propellant reduction with increasing flight time as do the true curves. Increasing the flight time much over 300 days is of limited value for decreasing propellant requirements. It is at this point that the increasing characteristic length tends to cancel the reducing effect of longer flight time on propellant consumption. The approximate curves in fact exhibit minimum values of J at flight times somewhat greater than 300 days; insufficient numerical data has been generated to confirm the existence of an optimal flight time for the actual trajectories.

Though the simple model seems to predict with reasonable accuracy the variation of J with flight time, the actual values so derived are generally considerably larger than the true values: errors of 60% or more are observed at the longer flight times. Such errors are to be expected. The rough agreement between characteristic length and the planetary separation distance generally deteriorates as flight times increase. For example, comparison of Figures 13 and 14 with Figure 17 indicates that the minimum L_c for

90-day VSI trajectories is only 5% less than the minimum L_g at opposition, but is 23% less than that value for 210-day transfers. Consequently the approximate minimum values of J derived from the planetary separation distance will be 10% and 50% larger, respectively, than the true values. The percent error in characteristic length is effectively doubled, since the J integral is proportional to L^2 for VSI missions, and is approximately so for CSI missions.

The observed errors in J do not, however, greatly limit the value of the averaged-trajectory model for calculating approximate propulsion requirements. For purposes of preliminary mission planning, a 60% or even a 100% error in the low values of a quantity that varies over a range of two or more orders of magnitude is not particularly serious, provided the general trend of the variation is reasonably accurate. Furthermore, since the percent error in J is large only for the long flight times when J is relatively small, the effect on final mass ratio is greatly reduced. This fact is evident from eq. (2-2), which can be rewritten as

$$\frac{m_f}{m_o} = \frac{1}{1 + \frac{J}{P}} \qquad (5\text{-}26)$$

The percent error in final mass ratio is approximately

$$\frac{\delta m_f}{m_f} \approx \frac{-\frac{J}{p}}{1+\frac{J}{p}} \frac{\delta J}{J} \qquad (5\text{-}27)$$

where m_f is the final mass ratio m_f/m_o. Thus when J is small compared to p, the error in J has little effect on the final mass ratio. This fact is illustrated in Figure 19a, where the final mass ratios for the cases under consideration are shown as functions of flight time; the ratio of power to initial mass is again

$$p=0.0242 \frac{kw}{kg}=0.6988 \times 10^{-6} \frac{au^2}{day^3}$$

The error in m_f is at most 5%, and only 2% at the longer flight times. The accuracy will, of course, improve with higher power ratios and deteriorate with lower ones.

5.4 Empirical Correction of Characteristic Length

The accuracy of propellant requirements calculated with the averaged-trajectory model can be greatly improved by the application of an empirical correction factor that better relates the true characteristic length of a trajectory to the planetary separation distance at mean trajectory time.

Close comparison of Figures 13 and 14 with Figure 17 indicates that minimum values of characteristic length (L_c) decrease with flight time for flight times up to about 270 days in very nearly the following fashion:

$$(t_f \leq 270) \qquad L_c^\circ \approx L_g^\circ \left[1 - 0.09\,(1 - \cos \bar{\omega} t_f)\right]$$

$$\approx L_g^\circ \left[1 - 0.18 \sin^2 \frac{\bar{\omega} t_f}{2}\right] \qquad (5\text{-}28)$$

where L_g is the planetary separation distance at opposition. The parameter $\bar{\omega}$ turns out to be almost exactly equal to the average of the mean angular motions of Earth and Mars:

$$\bar{\omega} \approx \frac{1}{2}(n_E + n_M) = 0.0132 \frac{rad}{day} \qquad (5\text{-}29)$$

For flight times greater than 270 days, eq. (5-28) does not yield accurate results. Better accuracy should be attainable with the expression

$$(t_f > 270) \qquad L_c^\circ \approx L_g^\circ \left[1 - 0.017\, \bar{\omega} t_f\right] \qquad (5\text{-}30)$$

Equations (5-28) and (5-30) are applicable only to the minimum values of characteristic length and planetary separation distance. The general discrepancy between L_c

and the corresponding L_g, i.e,

$$\Delta L(T_L, t_f) = L_g(T_L + t^*) - L_c(T_L, t_f) \tag{5-31}$$

varies in a rather complicated fashion as the launch date is moved farther from the optimum in either direction. For flight times less than 200 days, ΔL generally decreases as $|T_L - T_L^\circ|$ increases; for greater flight times, the converse is true. The variation can be described roughly by the expression

$$\frac{\Delta L(T_L, t_f)}{\Delta L^\circ(t_f)} \approx 1 - \frac{|T_L - T_L^\circ|}{0.35\, t_f}\left(1 - \frac{t_f}{200}\right) \tag{5-32}$$

where ΔL° is the discrepancy at the optimal launch date, given by (5-28) or (5-30). Combining eq. (5-32) with (5-28) or (5-30) yields the approximate empirical correction between the planetary separation distance at mean trajectory time and the true characteristic length:

$$\Delta L(T_L, t_f) \approx L_g^\circ\left(0.18 \sin^2 \frac{\bar{\omega} t_f}{2}\right)\left[1 - \frac{|T_L - T_L^\circ|}{0.35\, t_f}\left(1 - \frac{t_f}{200}\right)\right] \qquad t_f \le 270 \tag{5-33}$$

$$\approx L_g^\circ\left(0.017\, \bar{\omega} t_f\right)\left[1 - \frac{|T_L - T_L^\circ|}{0.35\, t_f}\left(1 - \frac{t_f}{200}\right)\right] \qquad t_f > 270 \tag{5-34}$$

The characteristic length is then

$$L_c(T_L, t_f) = L_g(T_L + t^*) - \Delta L(T_L, t_f) \tag{5-35}$$

The correction term, though a rather complicated addendum to an otherwise simple trajectory model, is nevertheless easily calculated when greater accuracy of predicted propellant requirements is desired. Only the mean angular velocities of the planets, plus the planetary positional data necessary to define the averaged trajectory, are required. Note, too, that

$$|T_L - T_L^\circ| = |T_L + t^* - T_{opp}| \tag{5-36}$$

To illustrate the improved accuracy resulting from application of the empirical correction term, the variation of propellant requirement with flight time for the sample VSI mission of Section 5.3 has been recalculated. Figure 19b compares the corrected values of J with the true values; the accuracy is much improved over the uncorrected values shown in Figure 6. Errors in J have been reduced from over 60% at the longer flight times to only 2% on the average. In general, however, such good agreement cannot be expected except when launch

dates are near the optimum for each flight time. The correction factor (5-32) is not accurate for large values of the ratio

$$\frac{|T_L - T_L^*|}{t_f}$$

Presumably launch dates that are near-optimal will be of the greatest interest to mission planning.

CHAPTER VI

MISSION PLANNING

6.1 General Remarks

The broad aspects of interplanetary mission planning have been discussed in Chapter I. The preliminary planning phase can generally be reduced to optimizing the mission on the basis of propellant expenditure. Propellant expenditure will be determined solely by the choice of propulsion system, launch date, and flight time; hence it is with these three design parameters that preliminary mission planning is primarily concerned. Both technical and non-technical constraints on the parameters require trade-off studies by which the best combination for a particular mission may be ascertained. In the past, trade-off studies have involved the generation of large quantities of trajectory data to evaluate the effects of parameter changes; for

low-thrust propulsion systems the process has been particularly time-consuming, requiring machine computation of an additional trajectory for each parameter change.

Preliminary analysis of interplanetary orbiter missions can be greatly facilitated by use of the averaged trajectory model developed in Chapter V. The model is specifically applicable to the heliocentric portion of two-body interplanetary trajectories matching the planetary positions and velocities at the end points. (Further applications of the model are discussed in Chapter VII.) The model is of particular value because of the ease with which the effects of parameter changes can be evaluated from the associated field-free space equations.

The averaged trajectory concept effectively implies that for each interplanetary mission, defined by a specific launch date and flight time, there exists a unique characteristic length. The characteristic length has been shown to be nearly invariant among and within the various propulsion modes, but to be directly related to the interplanetary geometry. Thus various propulsion systems can be compared and the effects of changing

propulsion parameters (power level and specific impulse) evaluated for each mission simply by applying the appropriate FFS equations to its particular characteristic length. Results will of course be approximate, but certainly will be accurate enough to reduce greatly the machine computation required to establish the optimum configuration.

6.2 Determination of Optimal Launch Dates

It is apparent from the preceding discussion that preliminary mission analysis can be focussed on determining the variation of characteristic length with launch date and flight time. It has been shown in previous chapters that an optimum launch date at which the characteristic length is locally minimized exists for any given flight time, and that this date occurs at approximately half the flight time prior to the subsequent opposition (or conjunction) of the planets in question. Thus the search for optimal launch dates may immediately be localized within the neighborhood of the first period of planetary alignment at which the mission will be technologically feasible.

For any given flight time, the optimum launch date can be determined to within a few days by the following procedure. First, the geometric separation distance between the launch and target planets must be obtained as a function of time near the date of planetary alignment. (For simplicity, consider an opposition.) For near-circular planetary orbits of small inclination, the minimum separation distance will occur essentially at that date. Next, the mean trajectory time t* for a typical trajectory of the specified flight time is calculated by the procedure described in Section 4.2. (This typical trajectory for best results should start at a launch date close to one half the flight time prior to opposition.) The optimum launch date is then very nearly equal to the opposition date minus the mean trajectory time so determined. Since the ratio of mean trajectory time to flight time is nearly independent of launch date or flight time for transfers (in the same direction) between near-circular orbits, the optimal launch dates for other flight times are easily calculated from the first.

Optimum launch dates can also be determined from reference trajectory data. Since the characteristic length of a particular trajectory is nearly independent of propulsion mode, it follows that the optimal launch date for each flight time will also be nearly independent of propulsion mode. Thus the characteristic lengths calculated, for example, from the ΔV of impulsive (ballistic) heliocentric trajectories may be used to establish the optimal launch dates for low-thrust trajectories of the same flight times. (Care must be taken, however, to ignore ballistic trajectory data corresponding to near-180 deg. transfer angles.) Thus the so-called "launch windows" for ballistic trajectories will in most cases apply as well to low-thrust trajectories.

6.3 Determination of Propellant Requirements

Once the characteristic length of a particular mission has been determined, the propellant requirements can be calculated from the appropriate FFS equations. Eqs. (3-2) to (3-4) relate the mission characteristic length to the ΔV, J, or m_f/m_o for impulsive, VSI, or CSI propulsion systems, respectively. ΔV and J are

themselves related to the final mass ratio by the equations

$$\text{(Impulsive)} \qquad \frac{m_f}{m_o} = e^{-\frac{\Delta V}{c}} \tag{6-1}$$

$$\text{(VSI and CSI)} \qquad \frac{m_f}{m_o} = \frac{1}{1 + \frac{J}{P}} \tag{6-2}$$

For quick calculation of approximate propellant requirements, the planetary separation distance L_g of the averaged trajectory for the mission may be used as the characteristic length. As discussed in Section 5.3, percent errors in the values of J calculated in this fashion for VSI or CSI trajectories will generally increase with longer flight times, being of the order of 10% for 90-day trajectories and 50% for 210-day transfers. However, these errors are greatly reduced in effect on the final mass ratio and corresponding propellant mass.

Considerably better accuracy may be achieved with the averaged trajectory model when the planetary separation distance L_g is modified by the empirical correction term developed in Section 5.4. For launch dates reasonably close (within 30 or 40 days) to the optimum values

for each flight time, errors in J can be reduced to less than 5%.

When ballistic trajectory data is available, the foregoing procedure for calculating characteristic lengths is unnecessary, except for missions of near-180 deg. transfer angles. Characteristic lengths can again be calculated without recourse to machine computation by applying eq. (3-2) to the ΔV's of the appropriate heliocentric trajectories. The averaged trajectory model is useful for determining which ballistic trajectories will yield the minimum characteristic lengths. In addition, for flight times greater than 120 days, the corrected planetary separation distance often approximates the low-thrust characteristic lengths better than do those of the corresponding ballistic trajectories.

When the characteristic length for a particular mission has been determined, high- and low-thrust propulsion systems can be compared on the basis of final payload capability. For high-thrust propulsion systems, the final mass includes useful payload plus structure and engine mass, where the latter are normally a small fraction of the initial mass. However, for power-limited

propulsion systems, the final mass ratio also includes the relatively large mass fraction of the powerplant. The useful payload is thus considerably smaller than the final mass of the spacecraft. Once the value of J for the mission is known, the powerplant can be sized according to eq. (1-3) so as to maximize the payload-plus-structure ratio, m_L/m_o. The maximum value of this ratio is given by eq. (1-4), repeated here for convenience:

$$\left(\frac{m_L}{m_o}\right)_{max} = \left(1-\sqrt{\alpha J}\right)^2 \tag{6-3}$$

where α is the powerplant specific mass, m_s/P. This ratio may be compared to that for the high-thrust system,

$$\frac{m_L}{m_o} = e^{-\frac{\Delta V}{c}} - \frac{m_e}{m_o} \tag{6-4}$$

where m_e is the engine mass. It is instructive to substitute the FFS equations (3-2) and (3-3) into (6-3) and (6-4), respectively, to obtain the payload ratio in terms of the mission characteristic length:

$$\text{(VSI)} \quad \left(\frac{m_L}{m_o}\right)_{max} = \left(1-\sqrt{\frac{6\alpha L^2}{t_f^3}}\right)^2 \tag{6-5}$$

$$\text{(Impulsive)} \quad \frac{m_L}{m_o} = e^{-\frac{2L}{ct_f}} - \frac{m_e}{m_o} \tag{6-6}$$

Because of the near-invariance of characteristic length with propulsion mode, eqs. (6-5) and (6-6) provide an easy means for comparing the maximum payload capability of low-thrust propulsion with that of high-thrust propulsion. Note that the most difficult missions that may be accomplished by either propulsion system in a given flight time are determined by the expressions

$$\text{(VSI)} \qquad L_{max} = \sqrt{\frac{t_f^3}{\alpha}} \qquad (6\text{-}7)$$

$$\text{(Impulsive)} \qquad L_{max} = \frac{1}{2} c t_f \ln \frac{m_o}{m_e} \qquad (6\text{-}8)$$

For low-thrust missions employing the more practical CSI propulsion system, values of J will be somewhat larger and payload capability smaller than those attained by VSI propulsion. To estimate the maximum payload capability of the CSI system for a particular mission, the mission planner may choose to optimize the specific impulse by the method of Section 5.2.

6.4 Mission Trade-Off Studies

The averaged trajectory concept and the associated FFS equations are most beneficial to the mission planner

in evaluating the trade-offs among the various design parameters that will determine the optimum mission. For example, the spacecraft design will generally be influenced by the flight time chosen for the mission. Longer flight times will usually require more redundant system design for increased reliability, greater fuel allotment for corrective maneuvers, increased shielding for radiation-sensitive components, and additional life-support equipment for the crews of manned spacecraft. All of these items will reduce the useful payload, or increase the initial mass, as the flight time is extended. To choose the best flight time for the mission, then, the mission planner must know at what rate increasing the flight time will reduce the propellant requirement and improve the final payload ratio. The answer is easily obtained to first-order accuracy by use of the averaged trajectory model and FFS equations.

As another example, one of the mission criteria might be to land an instrument package on Mars at the earliest date possible. Knowing the probable advancements in state-of-the-art propulsion systems as a function of launch date, the mission planner can with

the simple model calculate the earliest arrival date at which the mission can be accomplished with the desired final payload. The advances in propulsion technology and the specified final payload determine the maximum characteristic length capability as a function of launch date; the averaged trajectory model determines the minimum characteristic length requirement as a function of launch date and arrival date. The earliest possible arrival date is that at which the capability first equals the requirement.

It is evident that such trade-off studies would be prohibitively time-consuming if carried out by digital computer. The advantage of the averaged trajectory model is that it permits trade-off studies to be carried out by the application of simple FFS relationships to characteristic lengths defined as functions of launch date and flight time by the interplanetary geometry. Once the optimum mission parameters have been roughly determined by the simple model, relatively little machine computation is required to pin-point the accurate values.

A simple example of mission planning with the averaged trajectory technique is carried out in Appendix

C. The mission is a 100-day orbiter trajectory to Venus taking place in 1970. The optimal launch date is calculated and the best propulsion system chosen on the basis of payload capability. Numerically-computed trajectory data is also presented for comparison.

CHAPTER VII

SUMMARY AND CONCLUSIONS

7.1 Summary of the Investigation

The objective of this thesis has been to establish a correlation between the propulsion requirements and planetary positions related to an interplanetary trajectory, and thereby to develop a simple technique for preliminary mission planning based on the time-dependent interplanetary geometry.

The general aspects of interplanetary mission planning are discussed in Chapter I. For low-thrust missions, the search for optimum design parameters requires the generation of large amounts of trajectory data by digital computation; the process is both costly and time-consuming. Zola[15] has suggested that mission planning may be greatly expedited by the correlation of

trajectory propellant requirements among the various modes of rocket operation. The correlating parameter is the characteristic length of each trajectory, derived from the trajectory propellant requirements by the appropriate equation for a transfer in field-free space.

Chapter II presents the results of digital computer studies for the heliocentric portions of low-thrust "orbiter" trajectories between Earth and Mars near the 1971 opposition period. Actual planetary positions and velocities as functions of date are used as trajectory boundary conditions to determine the variation of propellant requirements with launch date and flight time. Ballistic trajectory data is also presented for sake of comparison.

The characteristic lengths derived from these propellant requirements are discussed in the third chapter. Characteristic lengths from the various propulsion modes are compared for a given mission. For different missions, the variation of characteristic length with launch date and flight time is analyzed and compared with the time-dependent separation distance between the launch and target planets. The significance of planetary alignments (oppositions or conjunctions) is noted.

Chapter IV develops the concept of mean trajectory time by which the characteristic lengths of interplanetary trajectories are correlated with the associated planetary separation distances. The mean trajectory time is interpreted on physical grounds, and a simple method by which it may be determined for any desired trajectory is presented.

The characteristic length, mean trajectory time, and planetary separation related to an interplanetary trajectory are combined in Chapter V to define an averaged trajectory in field-free space which closely approximates the propellant requirements of the actual transfer. Field-free space equations are then applied to averaged trajectories to calculate the optimal specific impulse for CSI propulsion, and to calculate the variation of propellant requirements with flight time from a fixed launch date. The corresponding digital computer results are presented for comparison. In addition, an empirical correction term is derived to improve the accuracy of actual propellant requirements calculated with the averaged trajectory model.

Application of the averaged trajectory model to preliminary mission planning is discussed in Chapter VI. Techniques are presented by which to estimate optimal launch dates for both ballistic and low-thrust trajectories, as well as to compare various propulsion systems on the basis of payload capability. Use of the simple model to study trade-offs between interrelated design parameters is described and compared to use of the digital computer.

A sample optimization is carried out in Appendix C for a mission to Venus.

7.2 Conclusions

The following general conclusions concerning propellant-optimal interplanetary trajectories may be drawn from the investigation:

1. The optimal launch dates for low-thrust interplanetary missions occur prior to the subsequent dates of planetary alignment by somewhat less than ½ the total flight time for radially-outbound trajectories, and by somewhat more than ½

the total flight time for radially-inbound trajectories.

2. Optimal launch dates for two-impulse ballistic trajectories are nearly the same as those for low-thrust trajectories of corresponding flight times, provided that heliocentric transfer angles are not near 180 deg.

3. Low-thrust trajectories between noncoplanar orbits incur no propellant penalties as the heliocentric transfer angle approaches 180 deg.

4. Low-thrust propulsion requirements for VSI trajectories decrease monotonically as the available flight time is increased, provided that the optimal launch date is chosen for each flight time.

5. For low-thrust missions starting from fixed launch dates, there will in some cases exist a finite optimal flight time.

6. An optimal specific impulse, or exhaust velocity, exists for every CSI mission; it is uniquely determined by the launch date, flight time, and power level.

7. The propellant requirements of each interplanetary mission may be reduced by field-free space equations to a characteristic length which is nearly independent of the propulsion system (observed previously by Zola).

8. The characteristic length is essentially a function only of launch date and flight time, and hence is unique for each mission; it is, in fact, roughly equal to the planetary separation distance at the mean trajectory time. The mean trajectory time is nearly half the flight time, and represents that time at which the spacecraft achieves the best average of its orbital energy and heliocentric travel angle over the transfer.

9. The propulsion requirements of an interplanetary trajectory can be approximated

by those of a unique averaged trajectory; the averaged trajectory is simply the rectilinear transfer in field-free space between the planetary positions at the mean trajectory time. The approximation is quite accurate when an empirical correction is applied to the planetary separation distance in question. The effects of various parameter changes on propulsion requirements can be estimated with good accuracy by applying the appropriate field-free space equations to the averaged trajectory.

10. The averaged trajectory model can be employed with good accuracy in the preliminary stages of mission planning to conduct trade-off studies and to evaluate optimum design parameters. Machine computation of trajectory data may thus be localized within a neighborhood of the simply derived optimum.

Items 8 to 10 represent the significant contributions of this thesis to the art of interplanetary mission planning.

7.3 Recommendations for Further Research

It has been previously noted that the averaged trajectory model derived in this thesis is applicable only to the heliocentric phase of interplanetary orbiter missions, for which terminal velocity conditions are fully specified. Relaxing the terminal velocity constraint is particularly pertinent to the analysis of fly-by trajectories, transfers to Mars via Venus, and atmospheric braking. The appropriate field-free space equations are easily developed and indicate that significant fuel savings may be achieved by relaxing terminal velocity constraints. It is thus recommended that the averaged trajectory technique be tested for fly-by missions and extended or modified, if necessary, so as to apply.

Once the effects of relaxed velocity constraints have been determined, the averaged trajectory model will be well-suited to the analysis of practical round-trip missions. The correlation of propellant requirements with the interplanetary geometry should greatly facilitate visualization and matching of inbound and outbound trajectories to find the best combination.

The planetary escape and capture phases of interplanetary missions may also permit simplified analysis in terms of characteristic length and field-free space equations; further investigation in this area is suggested.

The field-free space equations related to the averaged trajectory might also be applicable to analyzing the effects of various cost functions on "optimal" interplanetary trajectories. (For example, the cost might include a function of the total flight time, as well as the propellant expenditure.)

Another area relevant to mission planning is that of simple, non-optimal thrusting techniques for low-thrust trajectories. The optimal thrust programs of low-thrust trajectories near the date of planetary alignment often involve thrusting more or less in the direction of the target planet. Since guidance schemes based on thrusting directly toward the target planet at all times would be much simplified, it is recommended that research be conducted to determine the additional propellant cost of simplified thrusting techniques.

APPENDIX A

SPACE PROPULSION SYSTEMS

A.1 General Propulsion Relations

The thrust f produced by a rocket engine in space is given by the product of propellant mass flow rate $\dot{m}_p$ and the exhaust velocity c:

$$f = \dot{m}_p c \tag{A-1}$$

Note that $\dot{m}_p$ is considered to be a positive number, and is equal to the negative of the time rate of change of the overall spacecraft mass m:

$$\dot{m}_p = -\frac{dm}{dt} \tag{A-2}$$

The thrust acceleration a (often called the specific thrust) is then

$$a = \frac{f}{m} = \frac{\dot{m}_p}{m} c \tag{A-3}$$

The kinetic power P of the rocket exhaust is

$$P = \frac{1}{2} \dot{m}_p c^2 \qquad \text{(A-4)}$$

$$= \frac{1}{2} fc \qquad \text{(A-5)}$$

The specific exhaust power p is obtained by normalizing P with respect to the initial mass m_o:

$$p = \frac{P}{m_o} = \frac{1}{2} \frac{\dot{m}_p}{m_o} c^2 \qquad \text{(A-6)}$$

$$= \frac{1}{2} m a c \qquad \text{(A-7)}$$

where m is the normalized spacecraft mass

$$m = \frac{m}{m_o} \qquad \text{(A-8)}$$

The exhaust velocity is directly proportional to the specific impulse I_{sp} of the rocket; the proportionality factor is simply the standard earth gravity g. Thus

$$c = I_{sp} g \qquad \text{(A-9)}$$

A.2 High-Thrust Propulsion Systems

High-thrust propulsion systems may be defined as those devices producing thrust accelerations of the order of 0.1 g or greater. Generally only chemical rockets and some nuclear rockets will fall in this category. The final mass ratios attainable with high-thrust systems can be derived from the propellant mass flow rate. Combine equations (A-3) and (A-4) to yield

$$\frac{1}{m}\frac{dm}{dt} = \frac{d}{dt}(\ln m) = -\frac{a}{c} \tag{A-10}$$

When the exhaust velocity c is constant, eq. (A-10) can be integrated to yield

$$\ln \frac{m_f}{m_o} = -\frac{1}{c}\int_o^{t_f} |a|\, dt \tag{A-11}$$

where m_f is the final spacecraft mass and t_f the total flight time. The absolute value of a is employed to indicate that the magnitude of thrust acceleration, independent of direction, is the significant parameter. Define the ideal velocity increment ΔV as

$$\Delta V = \int_o^{t_f} |a|\, dt \tag{A-12}$$

Eq. (A-11) can then be rewritten as

$$\frac{m_f}{m_o} = e^{-\frac{\Delta V}{c}} \qquad \text{(A-13)}$$

Chemical rockets in general are characterized by constant exhaust velocity. The specific energy content of the propellant limits the exhaust velocity to about

$$c_{max} \approx 5000 \text{ m/sec}$$

for liquid-fuel rockets and about half that value for solid-fuel rockets. The exhaust power is limited only by the maximum mass flow rate of the rocket.

Nuclear rockets in general are capable of higher exhaust velocities in the range

$$c = 6000 \text{ to } 12{,}000 \text{ m/sec}$$

However, exhaust power is limited by the maximum power level of the nuclear power supply.

A.3 Power-Limited Propulsion Systems

Nuclear rockets and advanced electric (MHD, plasma-arc, and ion) rockets are generally characterized by the requirement of a separate power supply such as a nuclear reactor to provide energy to the propellant.

Consequently the exhaust power of the propellant is limited by the power level P_s of the power supply and the efficiency η of power conversion within the thrusting device:

$$P = \eta P_s \tag{A-14}$$

The final mass ratios attainable with power-limited propulsion systems are derived from eqs. (A-2) to (A-4); combine these to find

$$-\frac{1}{m^2}\frac{dm}{dt} = \frac{d}{dt}\left(\frac{1}{m}\right) = \frac{a^2}{2P} \tag{A-15}$$

When the power level of the power supply is constant, eq. (A-16) can be integrated to yield

$$\frac{m_o}{m_f} = 1 + \frac{m_o}{P_s}\int_o^{t_f} \frac{1}{\eta}\frac{a^2}{2}\,dt \tag{A-16}$$

The engine efficiency η will generally vary somewhat with exhaust velocity. For purposes of simplicity, however, consider it to be constant. Define the parameter J by the relation

$$J = \int_o^{t_f} \frac{a^2}{2}\,dt \tag{A-17}$$

(Many sources omit the factor of ½ in the definition.)

Then eq. (A-16) becomes

$$\frac{m_o}{m_f} = 1 + \frac{m_o J}{P} \qquad \text{(A-18)}$$

$$= 1 + \frac{J}{P} \qquad \text{(A-19)}$$

Thus maximizing the final mass m_f requires minimizing the J integral.

Since the powerplant mass m_s generally will compose a large fraction of the final spacecraft mass, the powerplant mass fraction must be sized to maximize the final useful payload ratio for a given mission. For this purpose, the spacecraft mass is considered to consist of essentially three parts: powerplant mass m_s, propellant mass m_p, and useful payload plus structure mass m_L. Thus

$$\frac{m_L}{m_o} = 1 - \frac{m_s}{m_o} - \frac{m_p}{m_o} \qquad \text{(A-20)}$$

For convenience, define α as the specific mass of the powerplant and β as the powerplant mass fraction:

$$\alpha = \frac{m_s}{P} = \frac{1}{\eta} \frac{m_s}{P_s} \qquad \text{(A-21)}$$

$$\beta = \frac{m_s}{m_o} \tag{A-22}$$

Then the specific power of the spacecraft is

$$p = \frac{\beta}{\alpha} \tag{A-23}$$

and equation (A-19) becomes

$$\frac{m_o}{m_f} = 1 + \frac{\alpha J}{\beta} \tag{A-24}$$

Note that the propellant mass ratio may be written

$$\frac{m_p}{m_o} = 1 - \frac{m_f}{m_o} = \frac{\frac{\alpha J}{\beta}}{1 + \frac{\alpha J}{\beta}} \tag{A-25}$$

Substitution of (A-22) and (A-25) into eq. (A-20) results in the following expression for the payload ratio:

$$\frac{m_L}{m_o} = \frac{1}{1 + \frac{\alpha J}{\beta}} - \beta \tag{A-26}$$

Differentiate eq. (A-26) with respect to β to find the value of β that maximizes m_L/m_o. The optimum value is

$$\beta_{opt} = \sqrt{\alpha J} - \alpha J \tag{A-27}$$

The corresponding maximum payload ratio is then

$$\left(\frac{m_L}{m_o}\right)_{max} = \left(1-\sqrt{\alpha J}\right)^2 \qquad \text{(A-28)}$$

The optimum specific power is found from eqs. (A-23) and (A-27) to be

$$p_{opt} = \sqrt{\frac{J}{\alpha}} - J \qquad \text{(A-29)}$$

Electric rockets contemplated for future space application appear capable of generating exhaust velocities over a very wide range[1],

$$c = 10{,}000 \text{ to } 600{,}000 \text{ m/sec}$$

At the higher specific impulses, or exhaust velocities, the resulting thrust accelerations will be very low because of the power limitations. Combining equations (A-7) and (A-23) determines the initial thrust acceleration to be

$$a_o = \frac{2p}{c_o} = \frac{2\beta}{\alpha c_o} \leq \frac{2}{\alpha c_o} \qquad \text{(A-30)}$$

The minimum powerplant specific masses expected within the next decade are about 4 kg/kw. For the range of exhaust velocities mentioned previously, the resulting

thrust accelerations will be of the order of 10^{-3} to 10^{-6} g's.

Current development of electric rockets indicate that any particular engine will probably be capable of only small variations in specific impulse. However, the unrestrained optimal acceleration program for low-thrust trajectories calls for variations in specific impulse by factors of 100 or more. Thus the VSI (variable specific impulse) propulsion mode represents an upper limit of low-thrust performance capabilities which in general will not be achieved in practice. The CSI (constant specific impulse) mode, on the other hand, much more closely represents the capabilities of practical systems, and will in fact establish a slightly conservative performance bound.

APPENDIX B

TRANSFERS IN FIELD-FREE SPACE

The dynamical relations for rocket-propelled transfers in field-free space are derived in this appendix for the three propulsion modes of interest: impulsive, VSI, and CSI. One-dimensional point-to-point transfers are analyzed, subject to the constraint that initial and terminal velocities be zero. These velocity constraints are analogous to those placed on interplanetary "orbiter" trajectories, for which the heliocentric velocities of the planets must be matched at the end-points.

B.1 Impulsive Transfers

The rectilinear distance to be travelled in FFS is denoted by L; the specified flight time is t_f. The spacecraft is accelerated impulsively from zero velocity at t = 0 to the velocity necessary to traverse the

distance L in time t_f. In the absence of external fields, that velocity will remain constant at the value

$$v = \frac{L}{t_f} \tag{B-1}$$

At the end of the trajectory the spacecraft must be decelerated impulsively to zero velocity. The two velocity impulses required are thus given by

$$\Delta v_1 = -\Delta v_2 = \frac{L}{t_f} \tag{B-2}$$

The total velocity increment ΔV required of the propulsion system is then

$$\Delta V = \int_0^{t_f} |a|\, dt = |\Delta v_1| + |\Delta v_2|$$

$$= \frac{2L}{t_f} \tag{B-3}$$

The final mass ratio of the spacecraft is determined by this value of ΔV and the exhaust velocity of the propulsion system according to eq. (A-13).

When the values of ΔV and t_f are given, the distance travelled is, from (B-3);

$$L = \frac{1}{2} \Delta V t_f \tag{B-4}$$

B.2 VSI Propulsion

The propellant-optimal acceleration program for a low-thrust trajectory is that which minimizes the integral

$$J = \int_0^{t_f} \frac{a^2}{2}\, dt \tag{B-5}$$

subject to the trajectory boundary conditions and any constraints on the acceleration. (For VSI transfers the acceleration is unrestricted.) The optimum acceleration program is found by the calculus of variations approach[3]. The problem is most easily set up in terms of the spacecraft velocity v. The thrust acceleration is then

$$a = \dot{v} \tag{B-6}$$

and the distance to be travelled is

$$L = \int_0^{t_f} v\, dt \tag{B-7}$$

The optimum velocity program is that which minimizes the functional

$$M = \int_0^{t_f} \frac{\dot{v}^2}{2}\, dt + \lambda \left(L - \int_0^{t_f} v\, dt \right)$$

$$= \lambda L + \int_0^{t_f} \left(\frac{\dot{v}^2}{2} - \lambda v \right) dt \tag{B-8}$$

where λ is an undetermined constant. Define the integrand as

$$F(v, \dot{v}) = \frac{\dot{v}^2}{2} - \lambda v \tag{B-9}$$

The variational calculus then specifies that the following Euler-Lagrange equation must be satisfied:

$$\frac{\partial F}{\partial v} - \frac{d}{dt}\left(\frac{\partial F}{\partial \dot{v}}\right) = 0 \tag{B-10}$$

Carrying out the indicated operation yields

$$\ddot{v} = -\lambda = \text{const.} \tag{B-11}$$

Integrating eq. (B-11) and applying the trajectory boundary conditions on position (x) and velocity, namely,

$$\left.\begin{matrix} x = 0 \\ v = 0 \end{matrix}\right\} \; t = 0 \tag{B-12}$$

$$\left.\begin{matrix} x = L \\ v = 0 \end{matrix}\right\} \; t = t_f \tag{B-13}$$

yields the following results:

$$a(t) = \frac{6L}{t_f^2}\left(1 - 2\frac{t}{t_f}\right) \tag{B-14}$$

$$v(t) = \frac{6L}{t_f}\left(\frac{t}{t_f}\right)\left(1 - \frac{t}{t_f}\right) \tag{B-15}$$

$$x(t) = L\left[3\left(\frac{t}{t_f}\right)^2 - 2\left(\frac{t}{t_f}\right)^3\right] \tag{B-16}$$

Note that the optimal acceleration program is simply a linear function passing through zero at the mid-point of the trajectory. The value of J obtained by substituting (B-14) into (B-5) is

$$J = \frac{6L^2}{t_f^3} \tag{B-17}$$

The final mass ratio of the spacecraft is determined from eq. (A-19) using this value of J and the specific power level p of the powerplant.

When J and the flight time are known, the distance travelled must be

$$L = \sqrt{\frac{J t_f^3}{6}} \tag{B-18}$$

The ideal velocity increment ΔV can be evaluated by integrating the absolute value of the acceleration given in eq. (B-15). The result is

$$\Delta V = \int_0^{t_f} |a| dt = \frac{3L}{t_f} \tag{B-19}$$

It is also of interest to derive the initial exhaust velocity called for by the optimal acceleration program. From eq. (A-7) the exhaust velocity is

$$c = \frac{2p}{am} \tag{B-20}$$

Substitution of eq. (B-14) into (B-20) and setting $t = 0$ then yields the initial value:

$$c_0 = \frac{p t_f^2}{3L} \tag{B-21}$$

B.3 CSI Propulsion

Point-to-point rectilinear transfers with CSI propulsion systems are completely deterministic when the exhaust velocity and power level are specified (L and t_f being fixed). No free parameter is left to be optimized, as in the case of VSI propulsion. Even the coast period is determined by the other

parameters. However, it will be shown that, when the exhaust velocity is not fixed, an optimum value for each mission may be derived.

Consider first the case in which c and p are both specified. Then the propellant mass flow rate and the thrust acceleration are determined from eqs. (A-3) and (A-4) to be

$$\dot{m}_p = \frac{2P}{c^2} \tag{B-22}$$

$$a = \frac{f}{m} = \frac{2P}{mc} \tag{B-23}$$

For simplicity, normalize m, $\dot{m}_p$, and P with respect to the initial mass m_o. Then (B-22) and (B-23) become

$$\dot{m}_p = \frac{2p}{c^2} \tag{B-24}$$

$$a = \frac{2p}{mc} = \frac{a_o}{m} \tag{B-25}$$

where the script m's denote the normalized variables and, as before, $p = P/m_o$. Note that $m_o = 1.0$. Since the propellant flow rate is constant by eq. (B-22), the time-varying mass can be written as

$$m(t) = 1 - \dot{m}_p t_{on} \tag{B-26}$$

where t_{on} does not include any coast periods. Then the acceleration magnitude by (B-25) is

$$a = \frac{a_o}{1 - \dot{m}_p t_{on}} \tag{B-27}$$

Consider the rocket to accelerate from t = 0 until $t = t_1$, then to coast from $t = t_1$ until $t = t_2$, and finally to decelerate from $t = t_2$ until $t = t_f$. The requirements that final velocity be zero and distance travelled be L will determine t_1 and t_2. Integrating eq. (B-27) yields the following velocities for each time period:

$$(t \le t_1) \qquad v(t) = -\frac{a_o}{\dot{m}_p} \ln (1 - \dot{m}_p t)$$
$$= -c \ln m(t) \tag{B-28}$$

$$(t_1 \le t \le t_2) \qquad v(t) = v_1 = -c \ln m_1 \tag{B-29}$$

$$(t_2 \le t \le t_f) \qquad v(t) = -c \ln m_1 + c \ln \frac{m(t)}{m_1} \tag{B-30}$$

Note that during each time period the mass is

$$\left.\begin{aligned} &(t \le t_1) \quad m(t) = 1 - \dot{m}_p t \\ &(t_1 \le t \le t_2) \quad m(t) = 1 - \dot{m}_p t_1 = m_1 \\ &(t_2 \le t \le t_f) \quad m(t) = m_1 - \dot{m}_p (t - t_2) \end{aligned}\right\} \tag{B-31}$$

Requiring that the final velocity be zero in eq. (B-30) determines the final mass ratio to be

$$m_f = m_1^2 \tag{B-32}$$

From eqs. (B-31) and (B-32) it can be shown that the ratio of the decelerating time $t_f - t_2$ to the accelerating time t_1 is

$$\frac{t_f - t_2}{t_1} = m_1 \tag{B-33}$$

Since the final mass ratio is

$$m_f = 1 - \dot{m}_p t_{on} \tag{B-34}$$

where $t_{on} = t_f - t_2 + t_1$, it is easily verified that the coast period Δt_c is given by

$$\Delta t_c = t_2 - t_1 = t_f - \frac{1 - m_1^2}{\dot{m}_p} \tag{B-35}$$

The distance travelled within the total flight time t_f is obtained by integrating the velocities (B-28) to (B-30) over the corresponding time intervals and summing the results. Specifying the total distance to be L determines m_1 (and hence m_f, t_1, t_2, and Δt_c) through the following transcendental equation:

$$L = -c t_f \ln m_1 + \frac{c^3}{2p}\left[(1-m_1)^2 + (1-m_1^2)\ln m_1\right] \qquad \text{(B-36)}$$

Eq. (B-36) may also be written in the form

$$L = -c\,\Delta t_c \ln m_1 + \frac{c^3}{2p}(1-m_1)^2 \qquad \text{(B-37)}$$

This second form provides a direct relationship between m_1 and L at the all-propulsion lower thrust limit, when $\Delta t_c = 0$.

Equation (B-36) cannot be solved explicitly for m_1 in terms of L, t_f, c, and p. Consequently explicit relations for J and ΔV also cannot be derived in terms of those parameters. However, J and ΔV may be evaluated in terms of m_1 by substituting (B-32) into (A-19) and (A-13), respectively, to yield

$$J = p\left(\frac{1-m_1^2}{m_1^2}\right) \tag{B-38}$$

$$\Delta V = -2c \ln m_1 \tag{B-39}$$

The optimum exhaust velocity for the transfer is that value which maximizes m_f or m_1 when the parameters L, t_f, and p have been specified. To determine this value, differentiate eq. (B-36) implicitly with respect to c and set

$$\frac{\partial m_1}{\partial c} = 0$$

The resulting equation,

$$L = -\frac{2}{3} c_{opt} t_f \ln m_{1(max)} \tag{B-40}$$

must be solved simultaneously with eq. (B-36) to determine c_{opt} and the maximum value of m_1.

Define an optimum exhaust velocity parameter $\mathcal{J}$ by the following relation:

$$\mathcal{J} = \frac{3L}{2 c_{opt} t_f} \tag{B-41}$$

Then (B-40) can be rewritten as

$$m_{1(max)} = e^{-\zeta}$$

(B-42)

Substituting (B-42) into eq. (B-36) results in a transcendental equation in the single variable ζ:

$$\frac{1}{D}\zeta^3 - (1-e^{-2\zeta})\zeta + (1-e^{-\zeta})^2 = 0$$

(B-43)

D is a mission "difficulty factor" defined as

$$D = \frac{27L^2}{8pt_f^3}$$

(B-44)

Note that larger values of L, smaller flight times, and lower power levels all constitute more difficult missions and produce larger values of D. When L, p, and t_f are given, D is evaluated from eq. (B-44). Then ζ is calculated by trial-and-error from eq. (B-43) using this value of D. Finally, the resulting value of ζ determines the optimum exhaust velocity from the relation

$$c_{opt} = \frac{1}{\zeta}\frac{3L}{2t_f}$$

(B-45)

APPENDIX C

EXAMPLE OF MISSION PLANNING

C.1 Description of the Mission

To illustrate application of the averaged trajectory model to preliminary mission planning, a sample optimization is carried out for an orbiter mission to Venus taking place sometime during 1970 or 1971. For simplicity, a fixed flight time of 100 days is assumed. It is desired to determine the optimum launch date, and to compare the payload capabilities of a present-day chemical rocket and a proposed electric rocket of variable specific impulse. The specific impulse of the chemical rocket is 400 sec.; the specific mass of the low-thrust powerplant is 4 kg/kw. Only the heliocentric portion of the total trajectory is considered.

C.2 Optimal Launch Date

It is known that the optimal launch date will occur at approximately half the flight time, or 50 days, prior to a conjunction of Earth and Venus occurring in 1970 or 1971. It is determined from Reference 16 that a conjunction occurs at J. D. 244 0900.8, or 10.3 November, 1970.

The optimal launch date will be determined by the mean trajectory time of a typical trajectory launched about 50 days prior to conjunction; the mean trajectory time for this trajectory is calculated by the method of Section 4.2. The radial distance of the Earth from the sun at J. D. 244 0850.8 is $r_L = 1.004$ a.u. That of Mars at J. D. 244 0950.8 is $r_T = 0.719$ a.u. By eq. (4-5) the radial distance of the average potential energy is

$$\bar{r} = \frac{2 r_L r_T}{r_L r_T} = 0.835 \text{ a.u.}$$

The fractional radial travel of the spacecraft to this point is

$$\frac{\Delta \bar{r}}{\Delta r_{tot}} = \frac{\bar{r} - r_L}{r_T - r_L} = \frac{-0.169}{-0.285} = 0.593$$

From Figure 18, find the corresponding ratio of mean trajectory time to total flight time:

$$\frac{t^*}{t_f} = 0.56$$

Thus the mean trajectory time is roughly 56 days; the optimal launch date then occurs approximately at

$$T^{\circ}_{L} = T_{conj} - t^* = \text{J. D. } 244\ 0844.5$$

As suggested at the end of Section 4.2, the position of average heliocentric angular momentum may also be significant in the determination of mean trajectory time. The position of average angular momentum is determined by averaging $r^{\frac{1}{2}}$ between the launch and target points. Performing this operation with the given values of r_L and r_T yields a somewhat different average radial distance:

$$\bar{r}' = 0.853 \text{ a.u.}$$

Repeating the preceding procedure yields the following results:

$$\frac{\overline{\Delta r}'}{\Delta r_{tot}} = \frac{\bar{r}' - r_L}{r_T - r_L} = \frac{-0.151}{-0.285} = 0.530$$

$$\frac{t^*}{t_f} = 0.52$$

$$T_L^\circ = \text{J. D. } 244\ 0848.5$$

The resulting optimal launch dates are reasonably close to one another. The actual value is probably somewhere in between; hence, assume the optimal launch date to be T_L° = J. D. 244 0846.5, and the mean trajectory time to be t* = 54 days.

C.3 Payload Capabilities

The characteristic length of the averaged trajectory corresponding to the optimal launch date is approximately equal to the planetary separation distance at the conjunction date; this value is L_g = 0.268 a.u. The empirical correction term developed in Section 5.3 may be applied to L_g in order to obtain a more accurate approximation to the actual minimum characteristic length. The corrected characteristic length is given by eq. (5-28):

$$L_c^\circ \approx L_g^\circ \left(1 - 0.18 \sin^2 \frac{\bar{\omega} t_f}{2}\right) \qquad \text{(C-1)}$$

where for this example $\bar{\omega}$ is equal to the average of the mean angular motions of Earth and Venus. These values

are, respectively, $n_E = 0.0172$ rad/day and $n_v = 0.0279$ rad/day. Thus, choose

$$\bar{\omega} = \tfrac{1}{2}(n_E + n_v) = 0.0226 \frac{\text{rad}}{\text{day}}$$

Substituting this value of $\bar{\omega}$ and $t_f = 100$ days into eq. (C-1) yields

$$L_c^\circ \approx L_g^\bullet (1 - 0.146) = 0.229 \text{ a.u.}$$

The propellant requirements of each propulsion mode can now be evaluated from L_c. For the chemical rocket, the required ideal velocity increment is evaluated from eq. (B-3) with $L = L_c^\circ$:

$$\Delta V = \frac{2L}{t_f} = 0.00458 \frac{\text{a.u.}}{\text{day}}$$

$$= 7950 \text{ m/sec}$$

The exhaust velocity corresponding to the specific impulse $I_{sp} = 400$ sec is

$$c = I_{sp}\, g = 3920 \text{ m/sec}$$

Then, from eq. (A-13), the final mass ratio is

$$\frac{m_f}{m_\circ} = e^{-\frac{\Delta V}{c}} = e^{-2.03} = 0.132$$

The final payload ratio is given by eq. (6-4) as

$$\frac{m_L}{m_\circ} = e^{-\frac{\Delta V}{c}} - \frac{m_e}{m_\circ} = 0.132 - \frac{m_e}{m_\circ}$$

The mass fraction m_e/m_o of the engine will be between 0.05 and 0.10. Taking the lower value, one finds the final payload ratio to be

$$\frac{m_L}{m_o} = 0.082$$

The payload ratio of the advanced propulsion system is evaluated next. Use $L = L_c^o$ again to determine J from eq. (B-17):

$$J = \frac{6L^2}{t_f^3} = 0.315 \times 10^{-6} \frac{au^2}{days^3}$$

$$= 0.0109 \frac{m^2}{sec^3}$$

The specific mass of the powerplant is α = 4 kg/kw. From eq. (A-28) the maximum payload ratio is then

$$\left(\frac{m_L}{m_o}\right)_{max} = \left(1 - \sqrt{\alpha J}\right)^2 = 0.625$$

To achieve the maximum payload ratio, the powerplant mass fraction β must be chosen to equal the optimum value given by eq. (A-27):

$$\beta_{opt} = \sqrt{\alpha J} - \alpha J = 0.165$$

The specific power level of the powerplant from eq. (A-23) is then

$$p = \frac{\beta}{\alpha} = 0.0413 \frac{kw}{kg}$$

It is evident by comparison of the final payload capability of the two propulsion systems that the low-thrust VSI rocket is far superior to the chemical rocket for the desired mission to Venus.

C.4 Comparison with Computer Results

Figure 20 shows the variation of characteristic length with launch date for actual ballistic and VSI trajectories to Venus. Note that the optimum launch date is essentially the same as that determined by the simple model. The minimum values of characteristic length are

$$\text{(Impulsive)} \qquad L_c^\circ = 0.242 \text{ a.u.}$$

$$\text{(VSI)} \qquad L_c^\circ = 0.234 \text{ a.u.}$$

The empirically corrected value from the simple model is thus about 5% too low for the impulsive trajectory and 2% too low for the VSI trajectory. The minimum values of ΔV and J are

$$\Delta V = 0.00485 \ \frac{\text{au}}{\text{day}} = 8420 \text{ m/sec}$$

$$J = 0.329 \times 10^{-6} \ \frac{\text{au}^2}{\text{day}^3} = 0.0114 \ \frac{\text{m}^2}{\text{sec}^3}$$

The corresponding final payload ratios are

(Impulsive) $$\frac{m_L}{m_o} = 0.117 - \frac{m_e}{m_o} = 0.067$$

(VSI) $$\left(\frac{m_L}{m_o}\right)_{max} = 0.619$$

The accurate computer results are in particularly good agreement with those of the averaged trajectory model for the low-thrust trajectory.

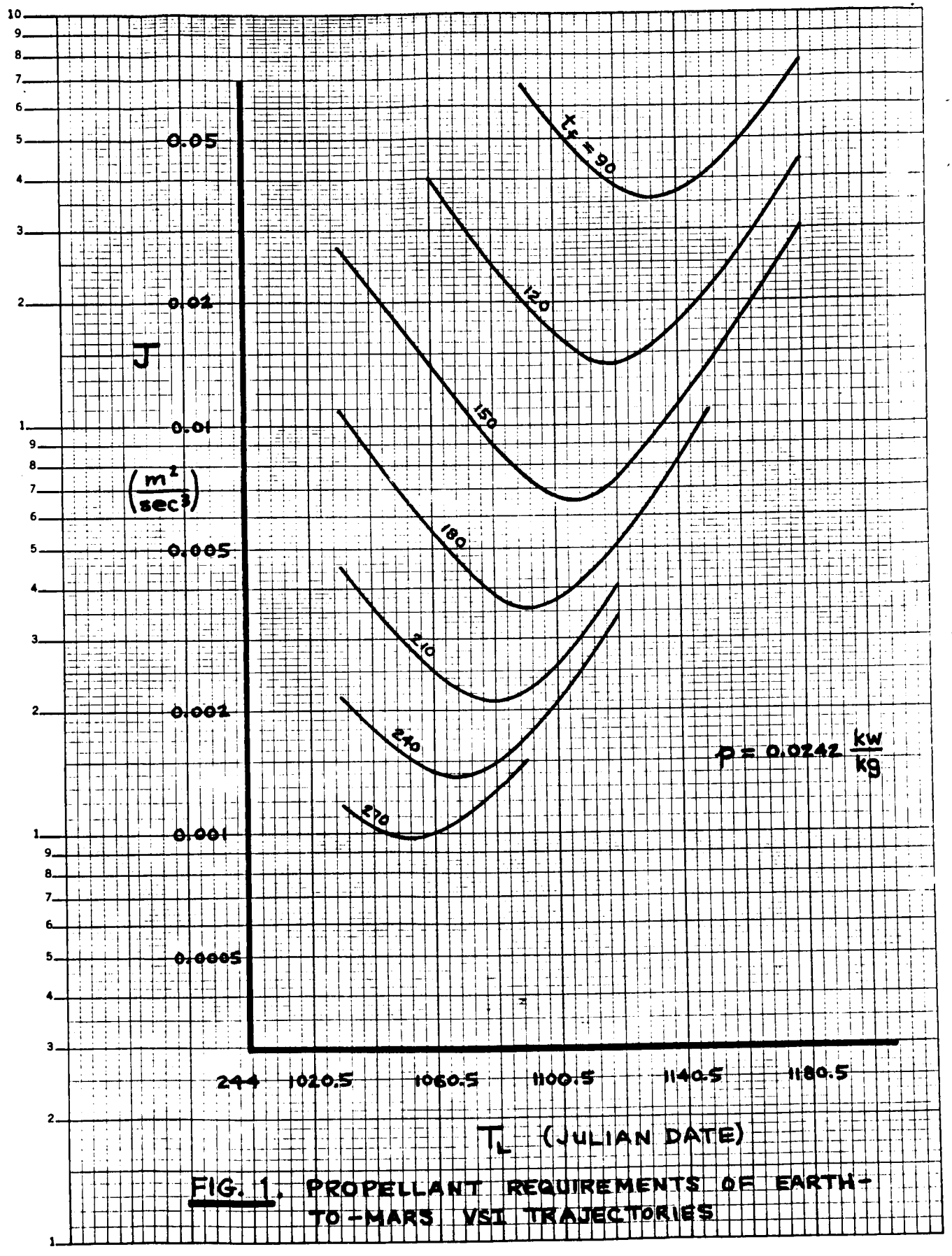

FIG. 1. PROPELLANT REQUIREMENTS OF EARTH-TO-MARS VSI TRAJECTORIES

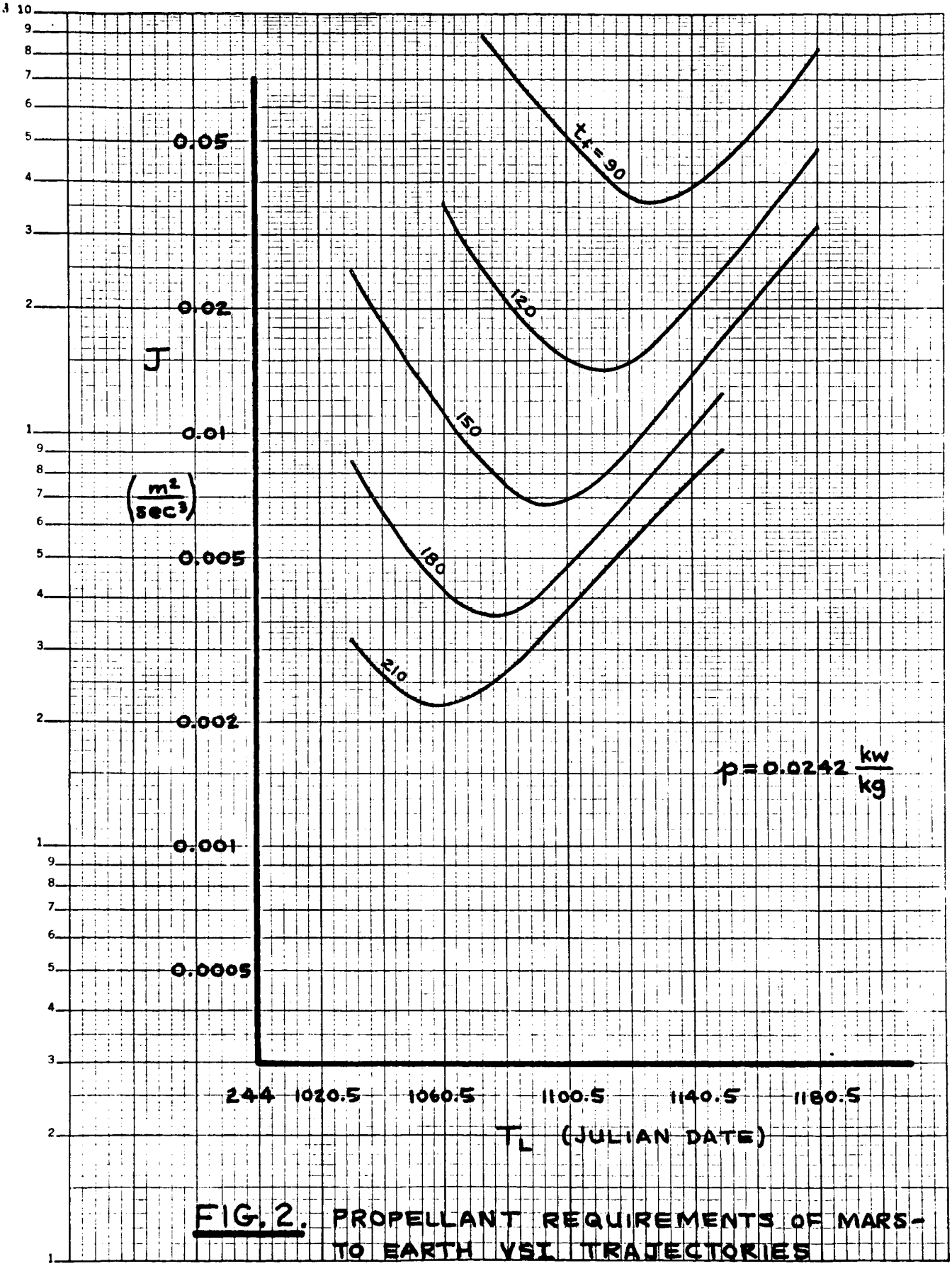

FIG. 2. PROPELLANT REQUIREMENTS OF MARS-TO EARTH VSI TRAJECTORIES

Semi-Logarithmic
3 Cycles x 10 to the inch

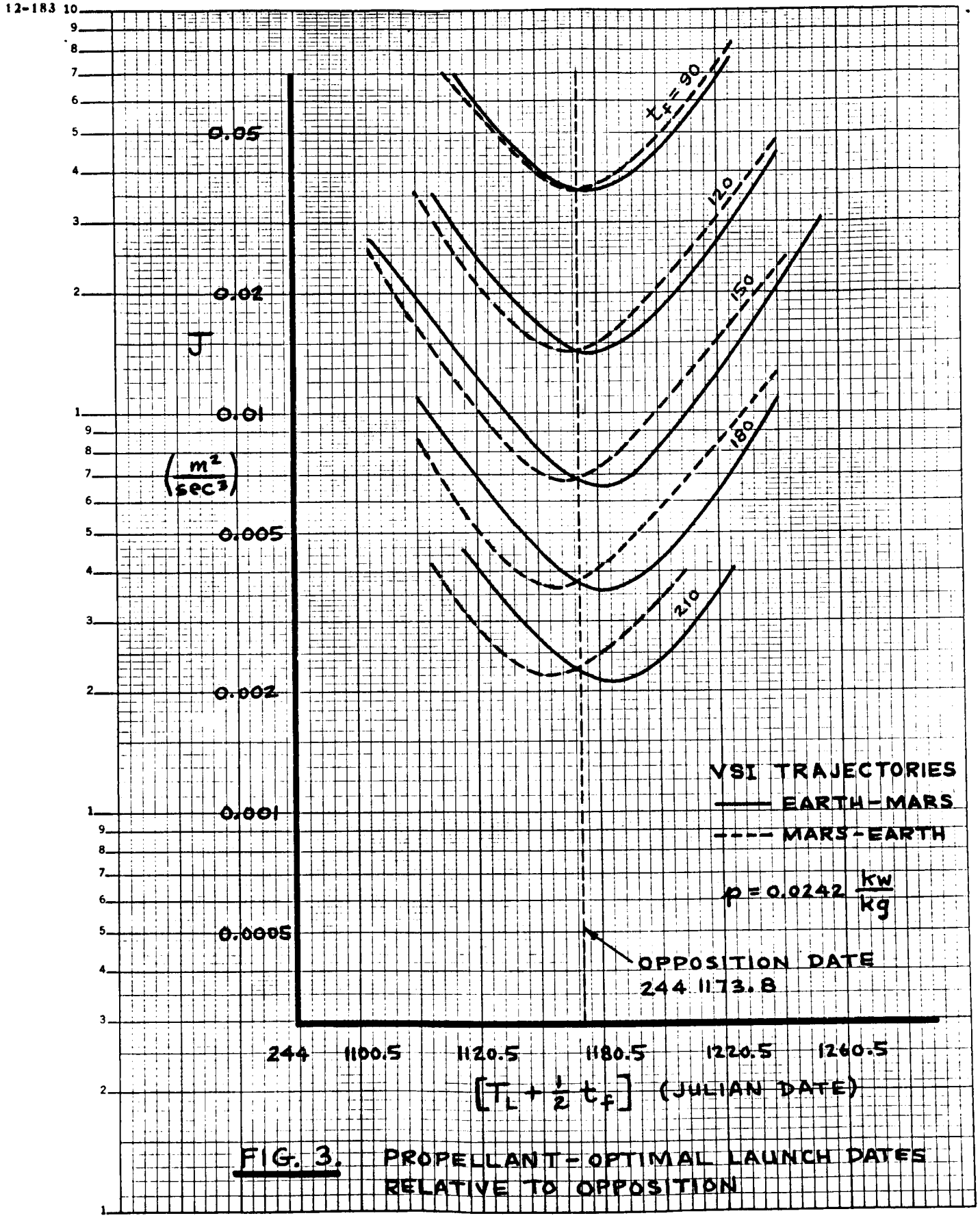

FIG. 3. PROPELLANT-OPTIMAL LAUNCH DATES RELATIVE TO OPPOSITION

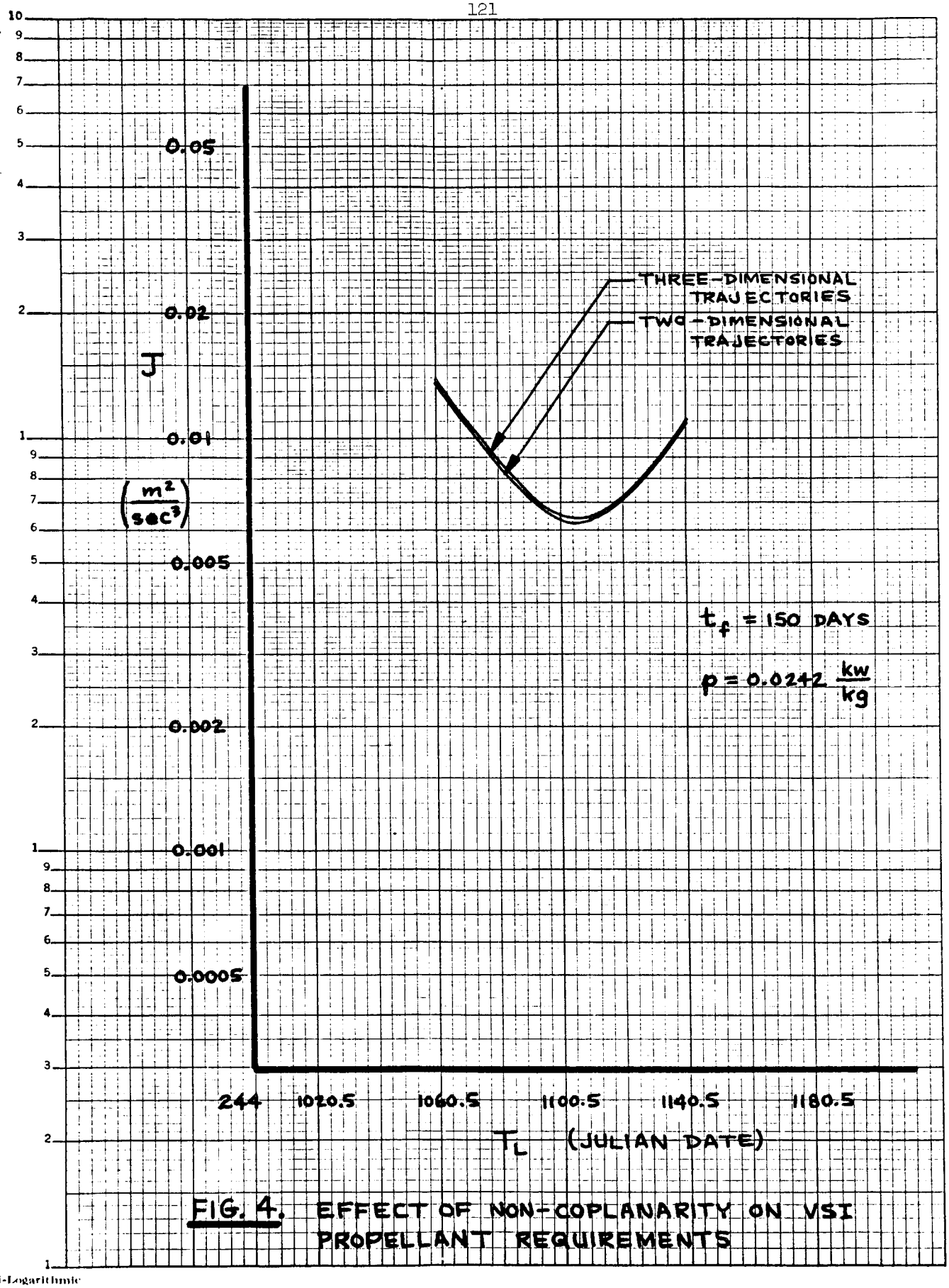

FIG. 4. EFFECT OF NON-COPLANARITY ON VSI PROPELLANT REQUIREMENTS

Semi-Logarithmic
3 Cycles x 10 to the inch

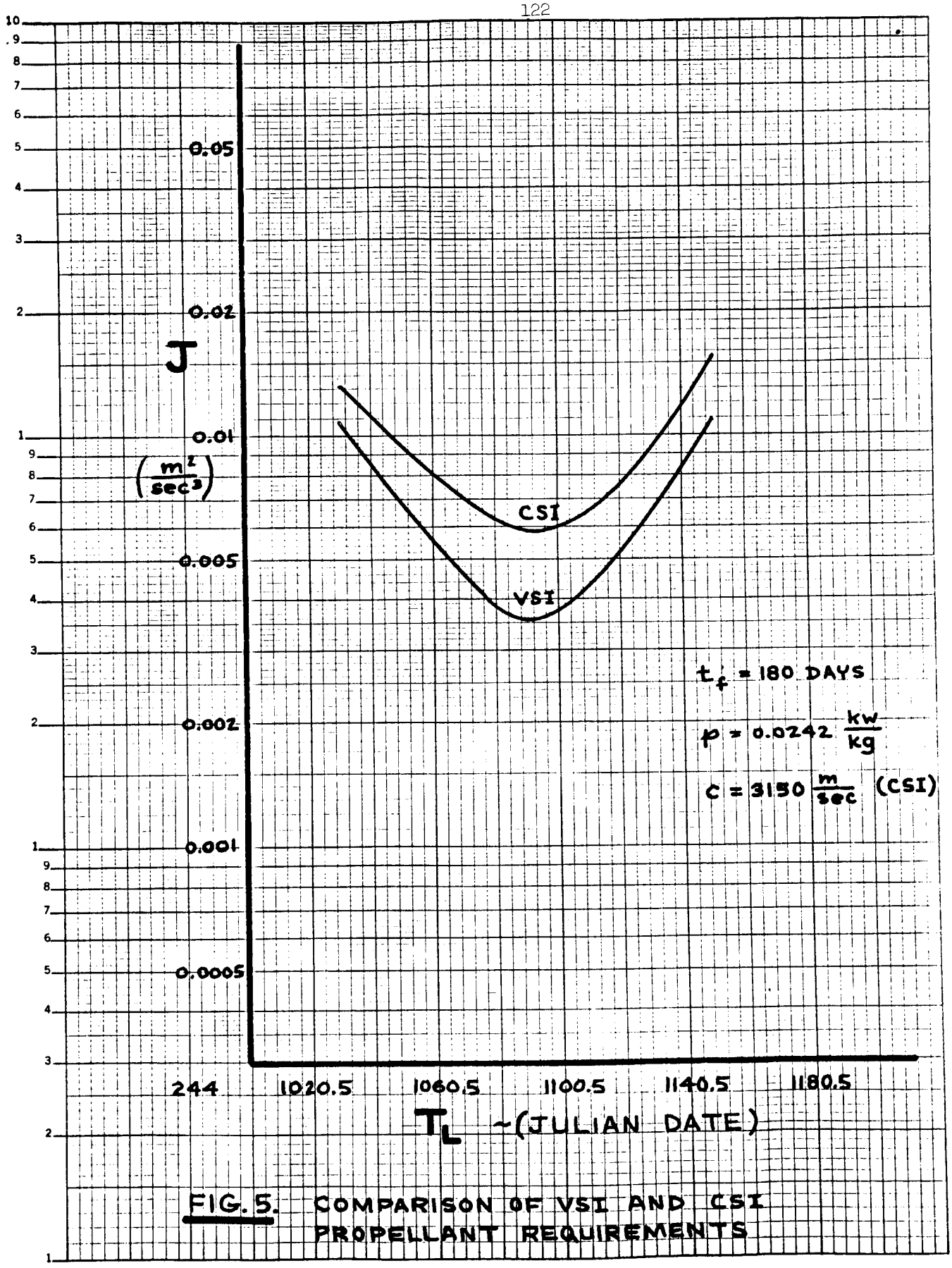

FIG. 5. COMPARISON OF VSI AND CSI PROPELLANT REQUIREMENTS

Semi-Logarithmic
3 Cycles x 10 to the Inch

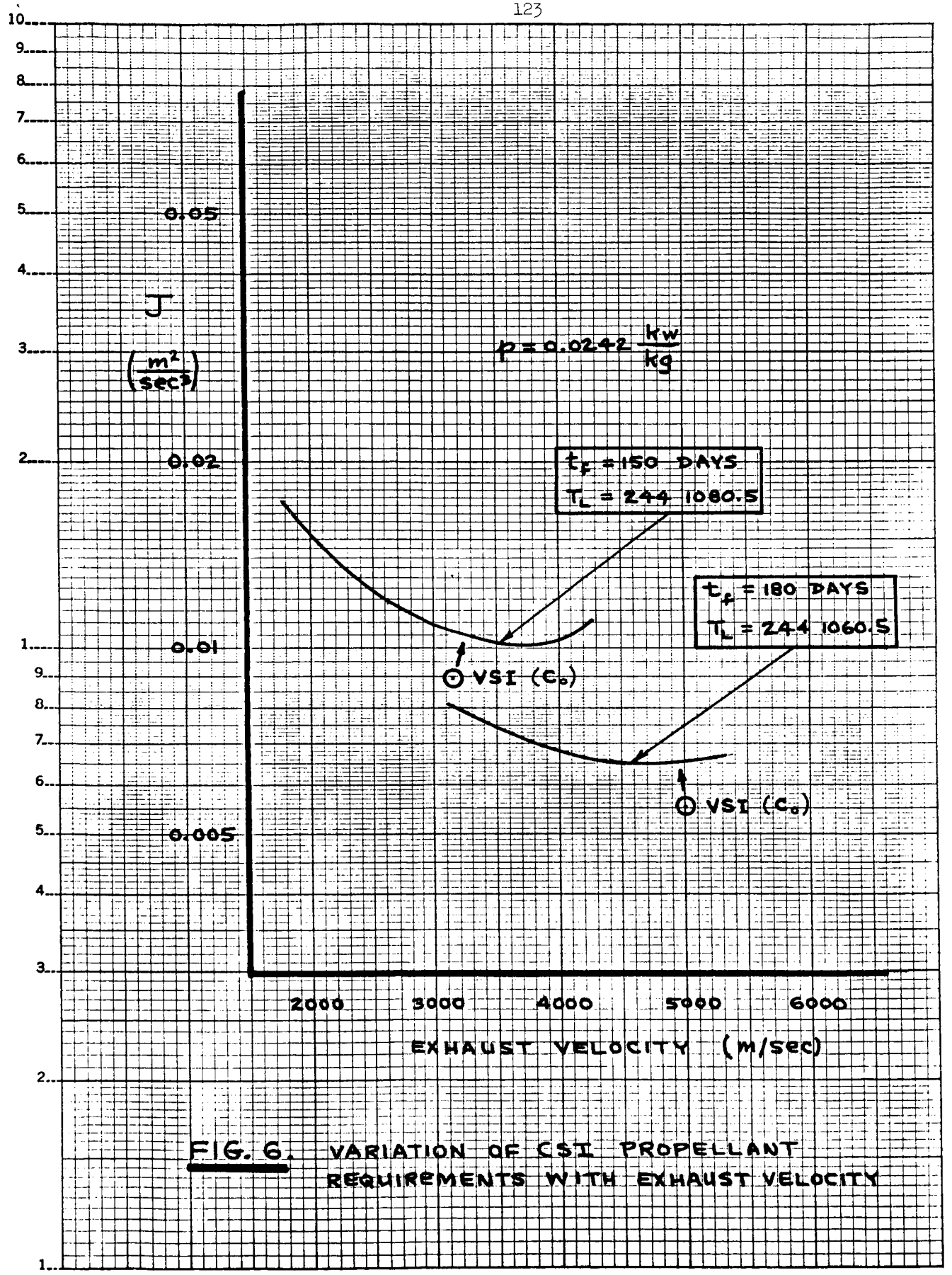

FIG. 6. VARIATION OF CSI PROPELLANT REQUIREMENTS WITH EXHAUST VELOCITY

Semi-Logarithmic
2 Cycles x 10 to the inch

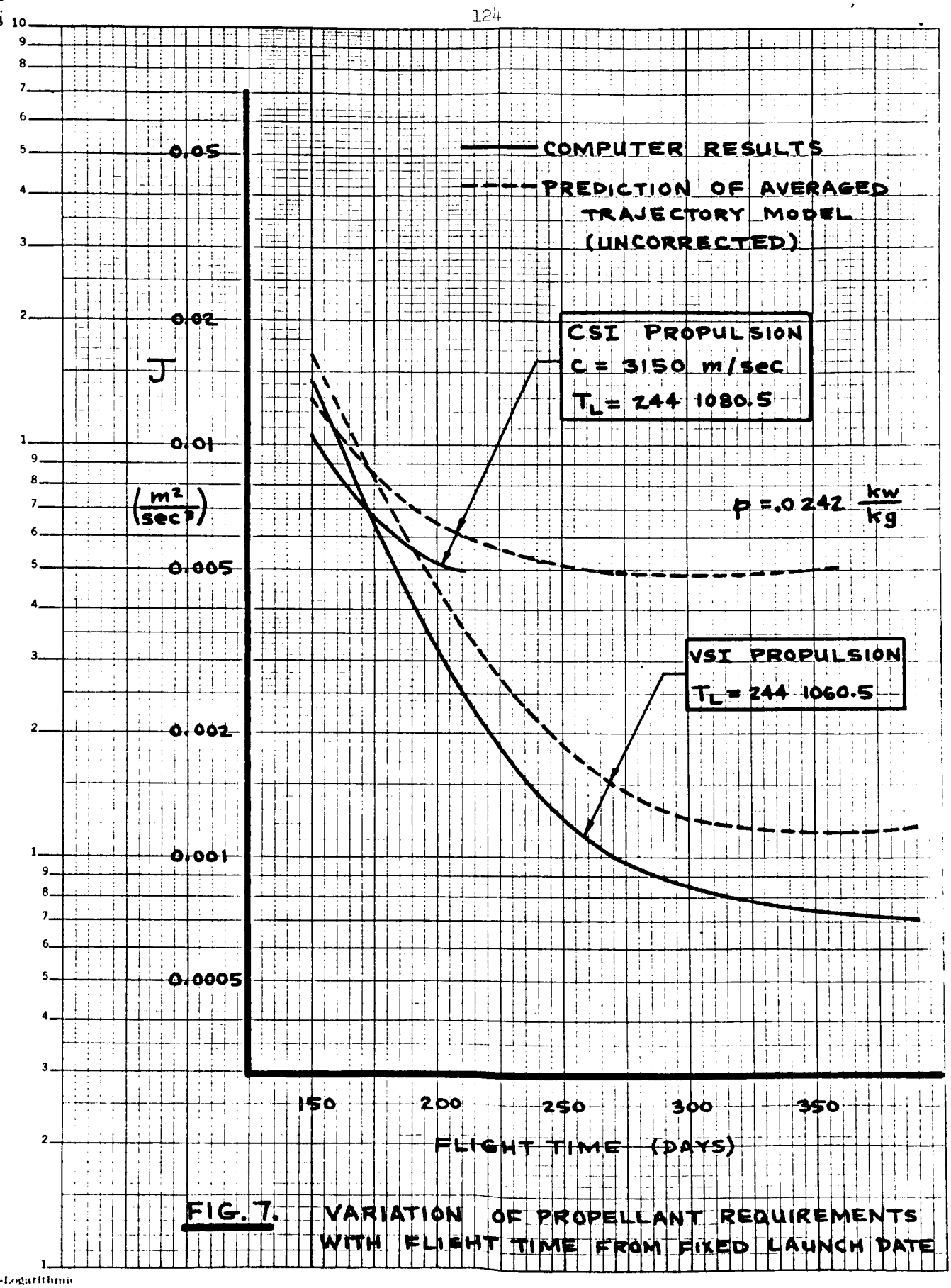

FIG. 7. VARIATION OF PROPELLANT REQUIREMENTS WITH FLIGHT TIME FROM FIXED LAUNCH DATE

Semi-Logarithmic
3 Cycles x 10 to the Inch

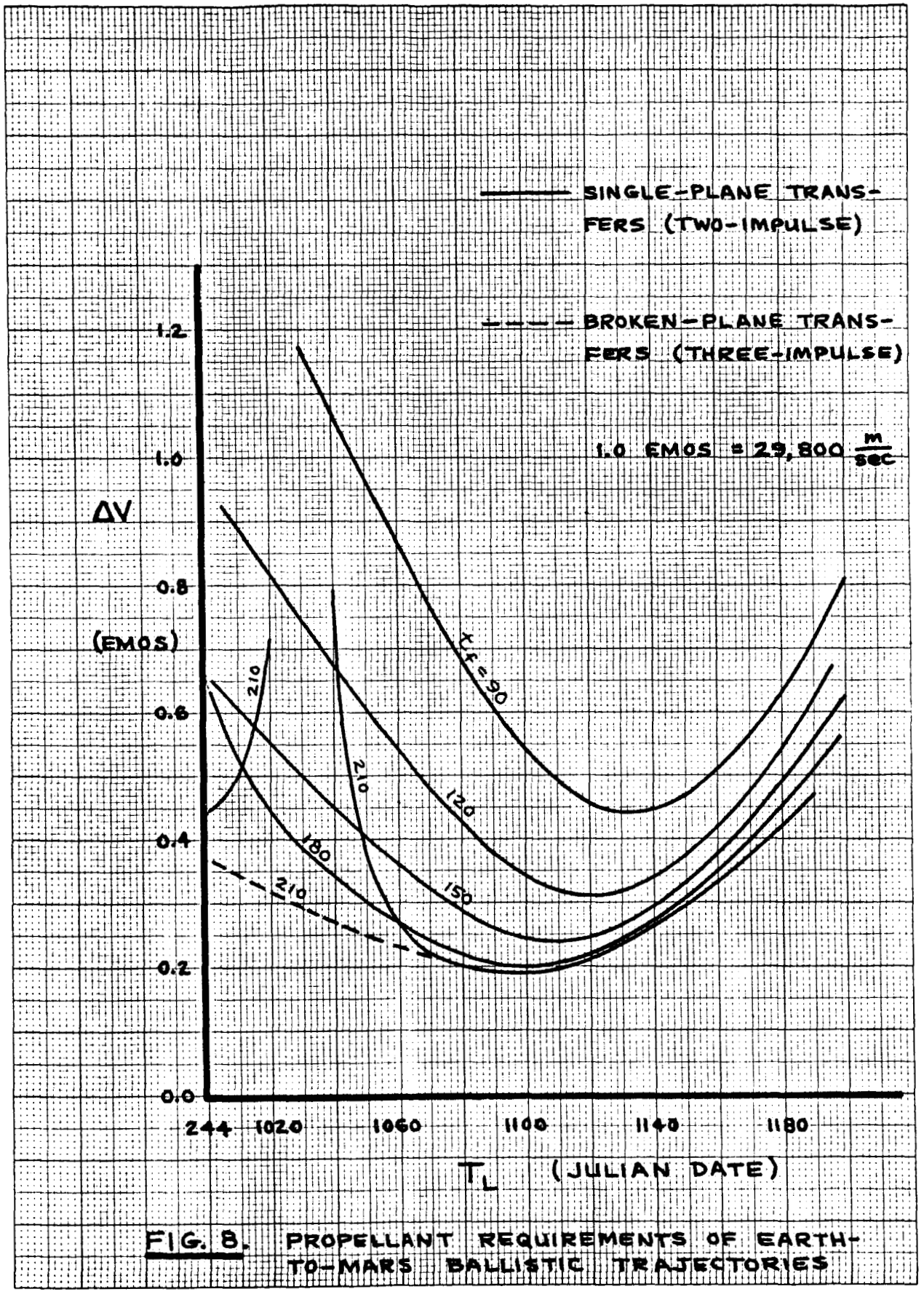

FIG. 8. PROPELLANT REQUIREMENTS OF EARTH-TO-MARS BALLISTIC TRAJECTORIES

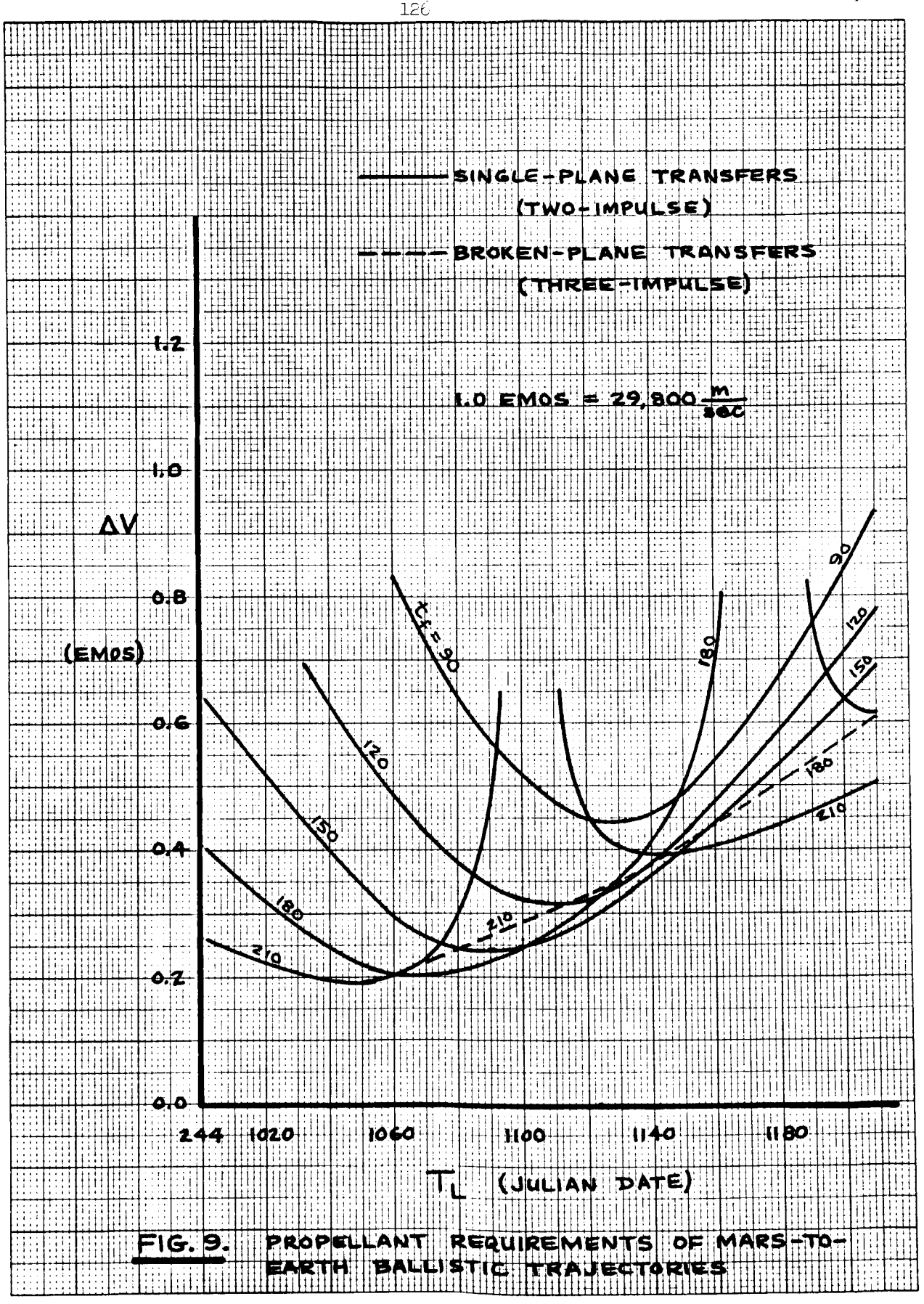

FIG. 9. PROPELLANT REQUIREMENTS OF MARS-TO-EARTH BALLISTIC TRAJECTORIES

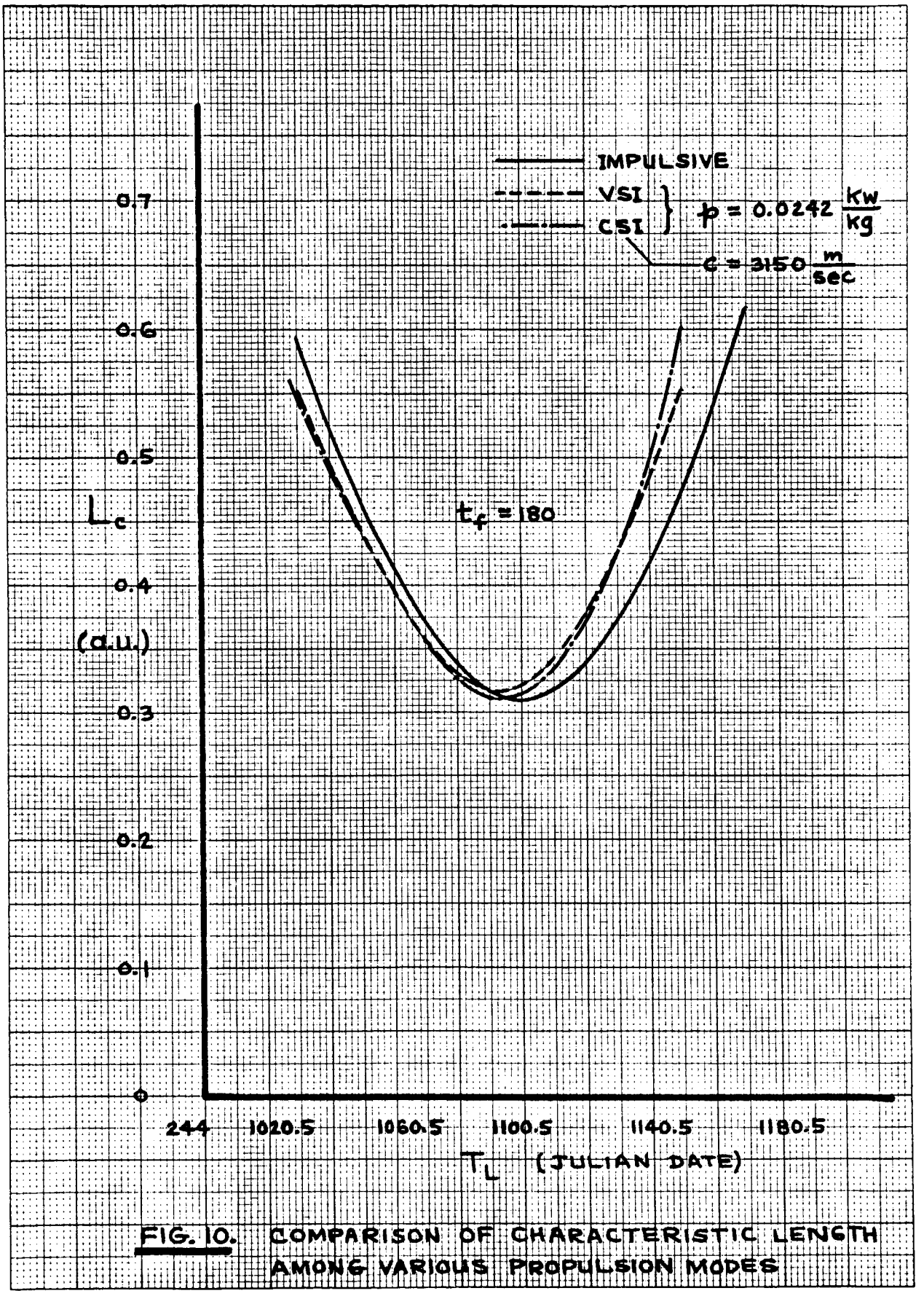

FIG. 10. COMPARISON OF CHARACTERISTIC LENGTH AMONG VARIOUS PROPULSION MODES

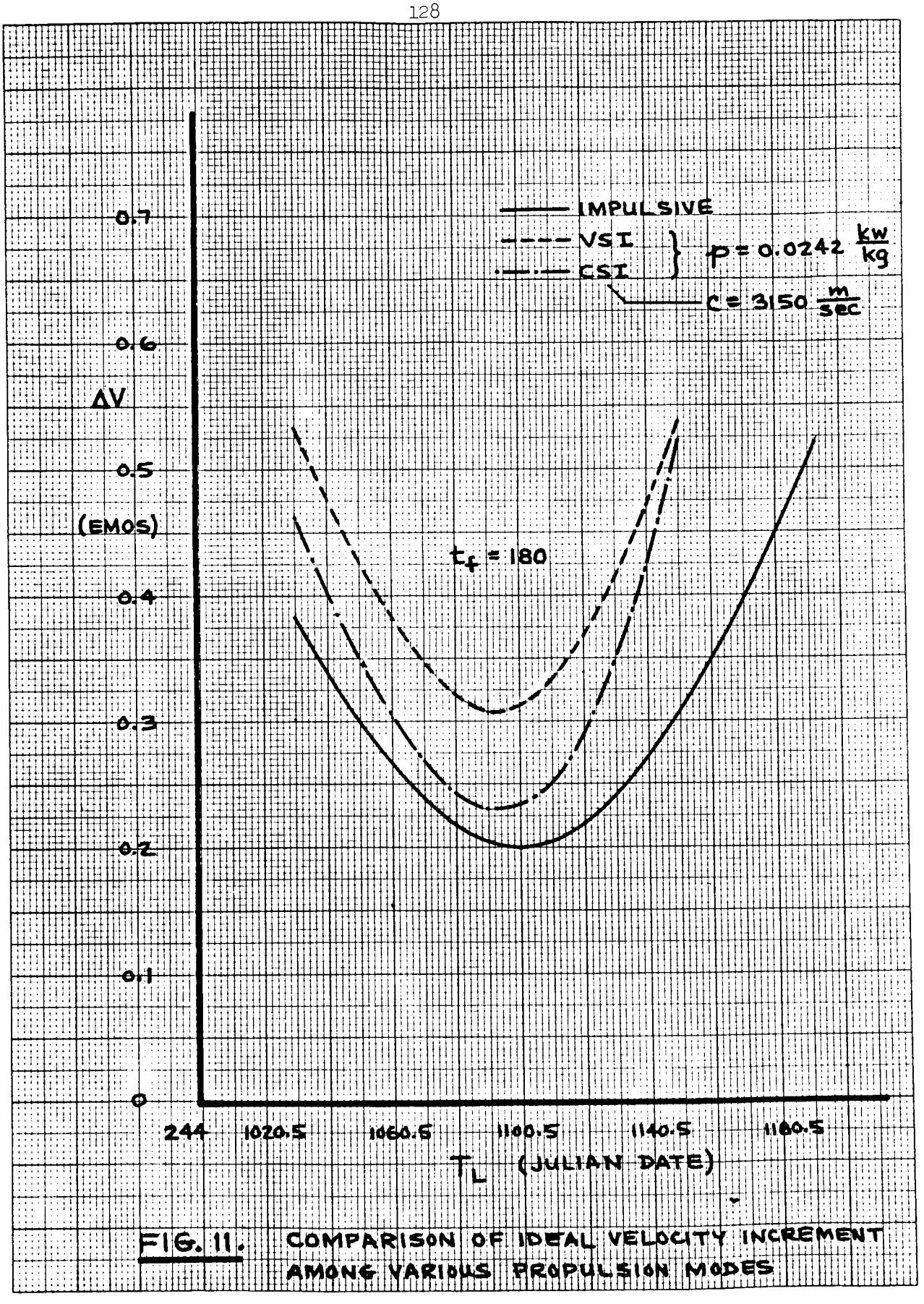

FIG. 11. COMPARISON OF IDEAL VELOCITY INCREMENT AMONG VARIOUS PROPULSION MODES

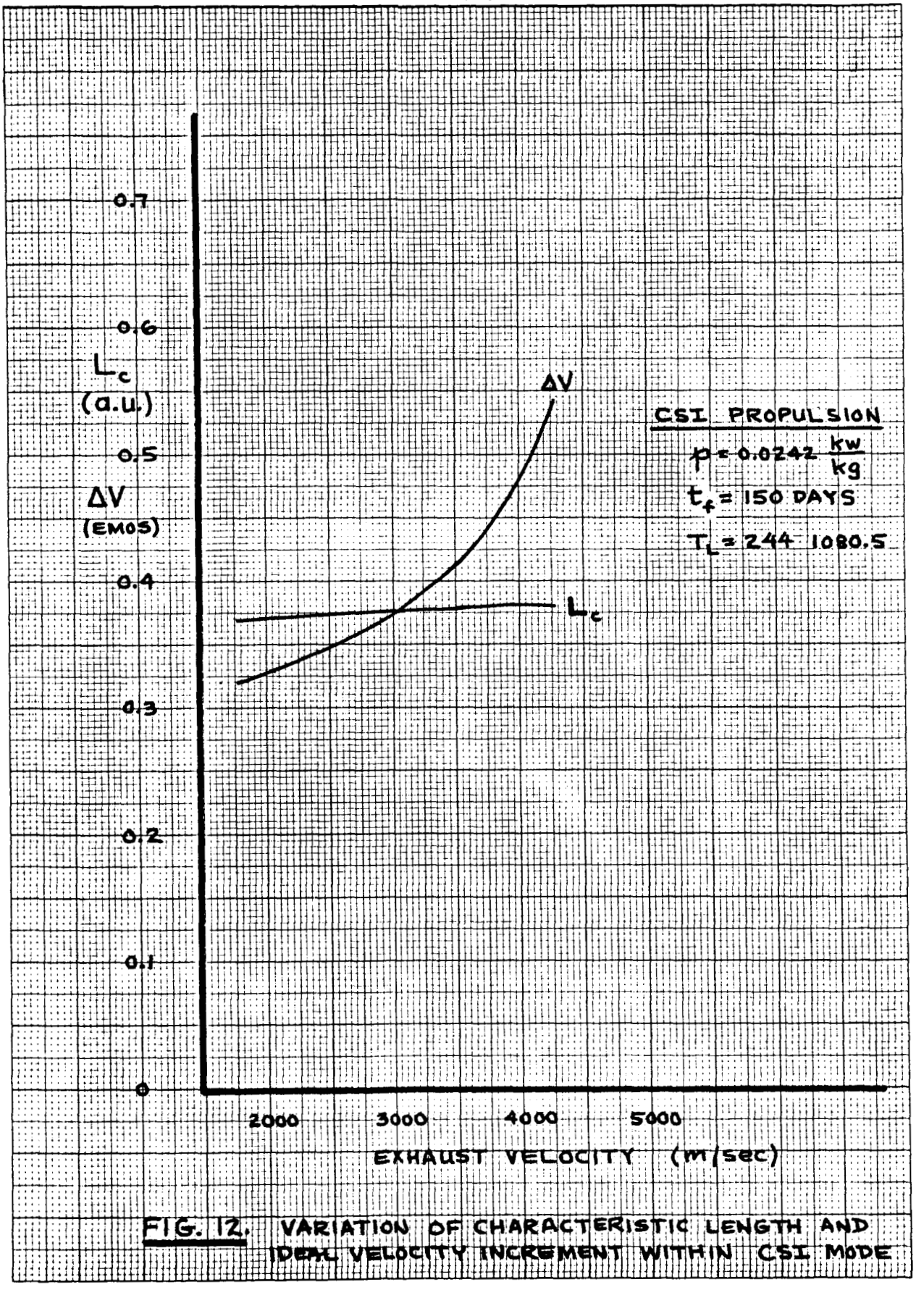

FIG. 12. VARIATION OF CHARACTERISTIC LENGTH AND IDEAL VELOCITY INCREMENT WITHIN CSI MODE

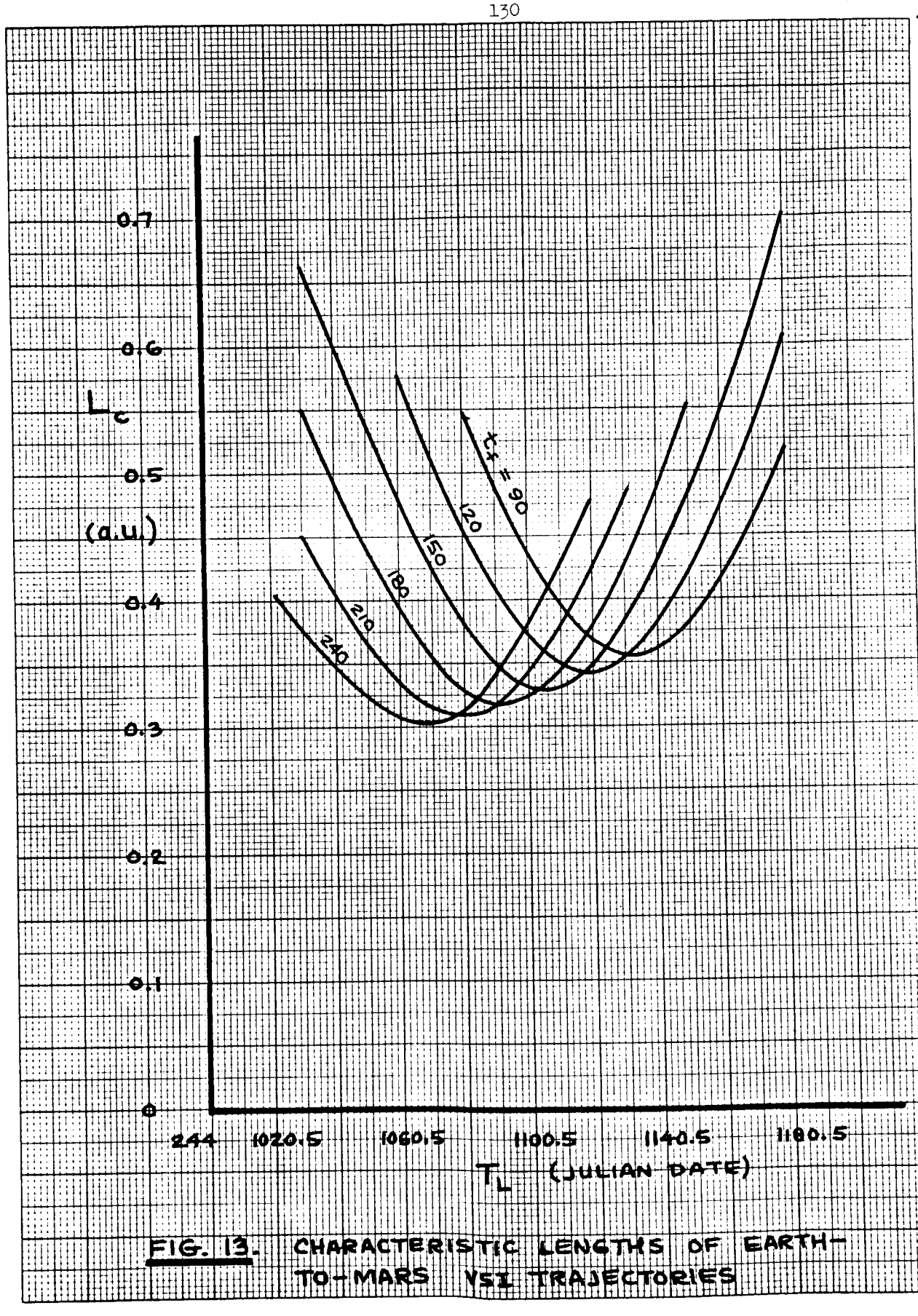

FIG. 13. CHARACTERISTIC LENGTHS OF EARTH-TO-MARS VSI TRAJECTORIES

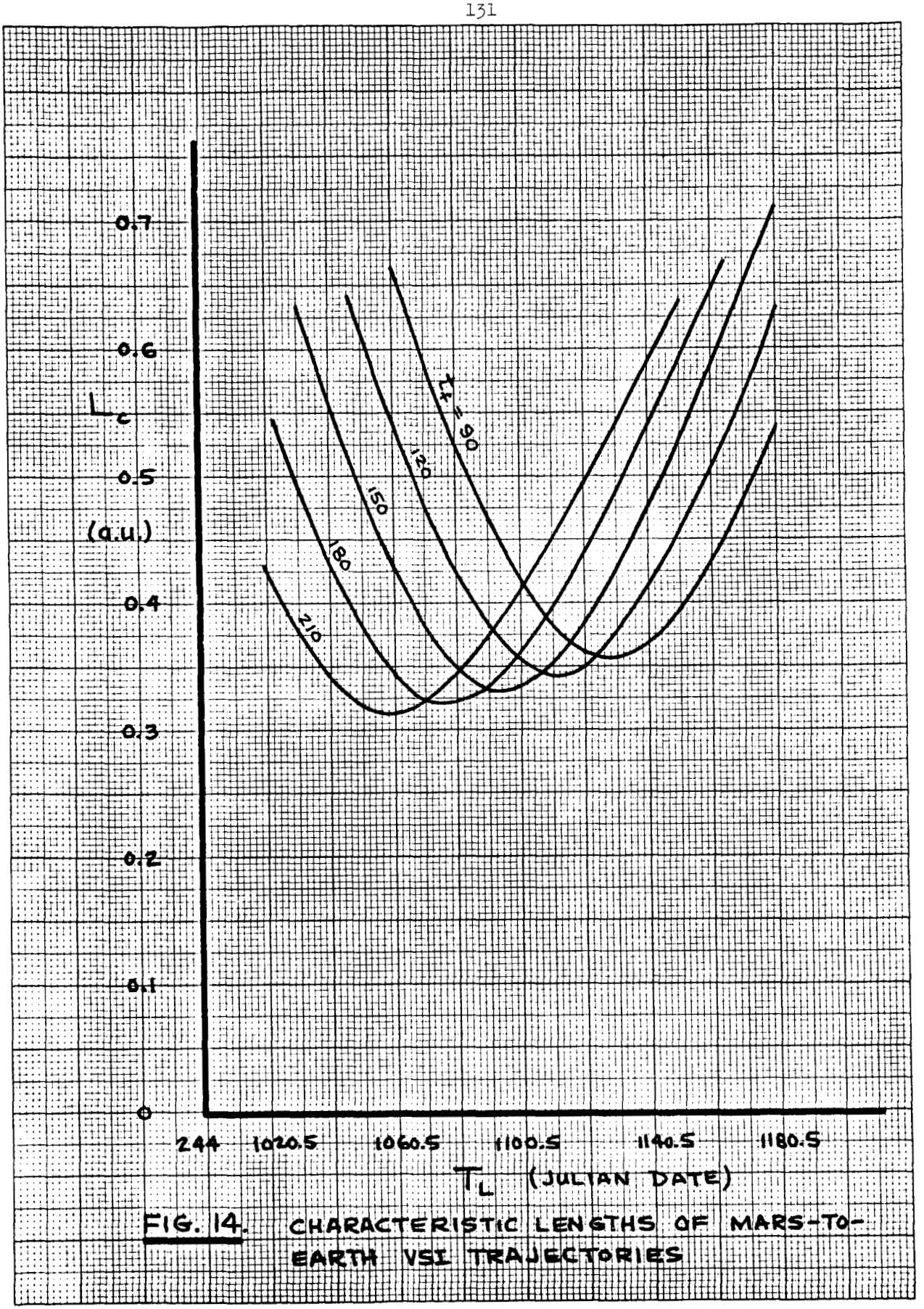

FIG. 14. CHARACTERISTIC LENGTHS OF MARS-TO-EARTH VSI TRAJECTORIES

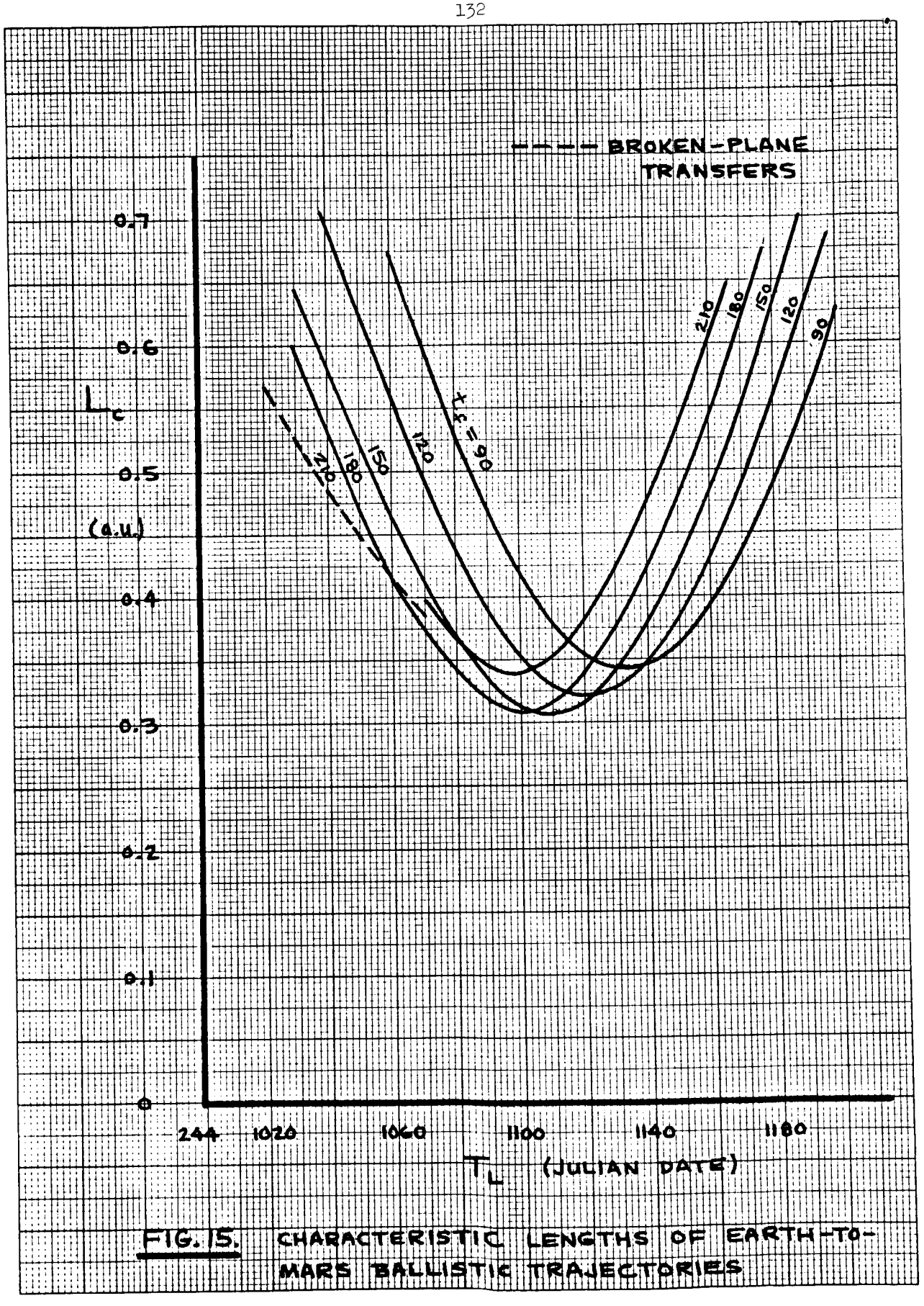

FIG. 15. CHARACTERISTIC LENGTHS OF EARTH-TO-MARS BALLISTIC TRAJECTORIES

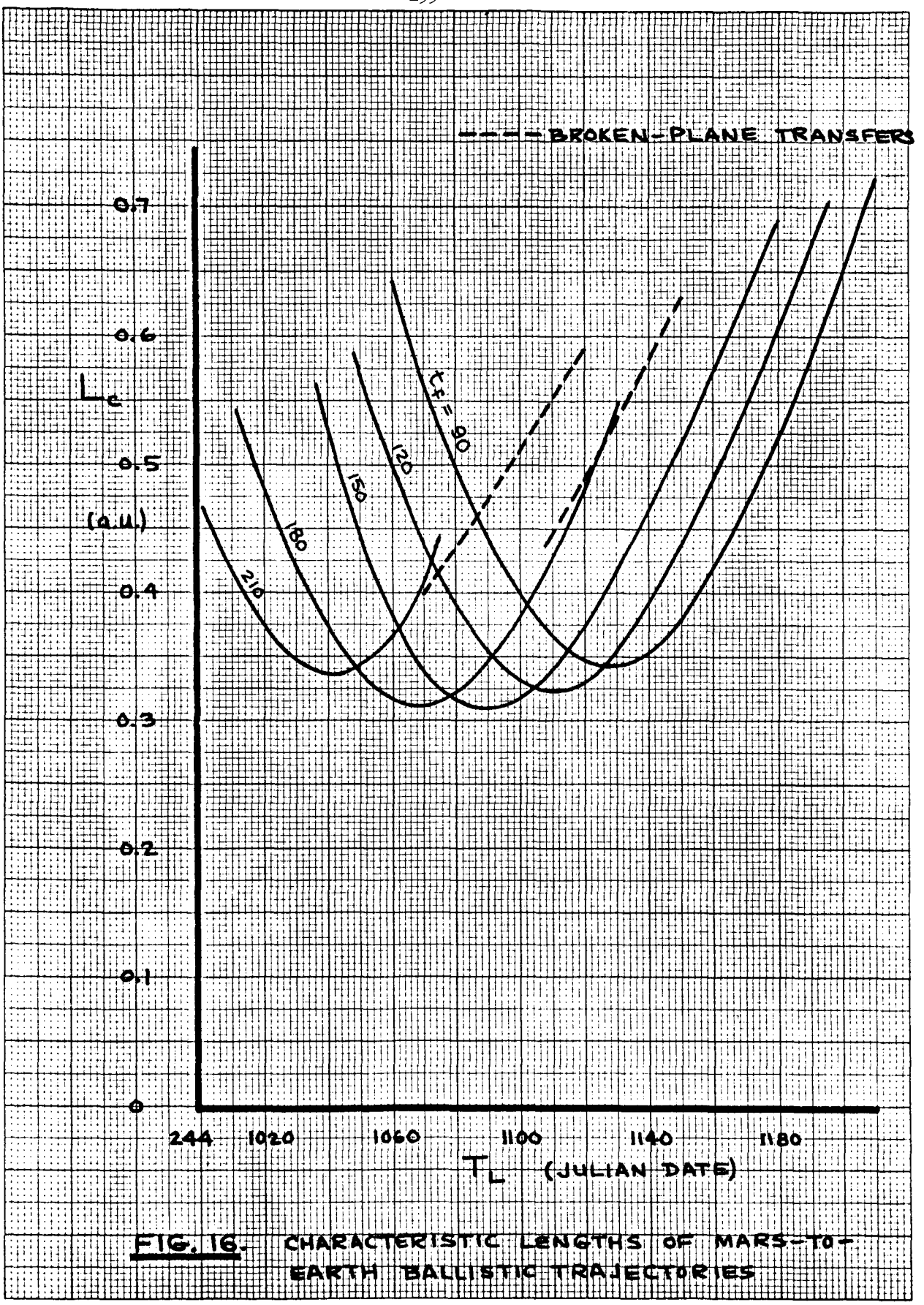

FIG. 16. CHARACTERISTIC LENGTHS OF MARS-TO-EARTH BALLISTIC TRAJECTORIES

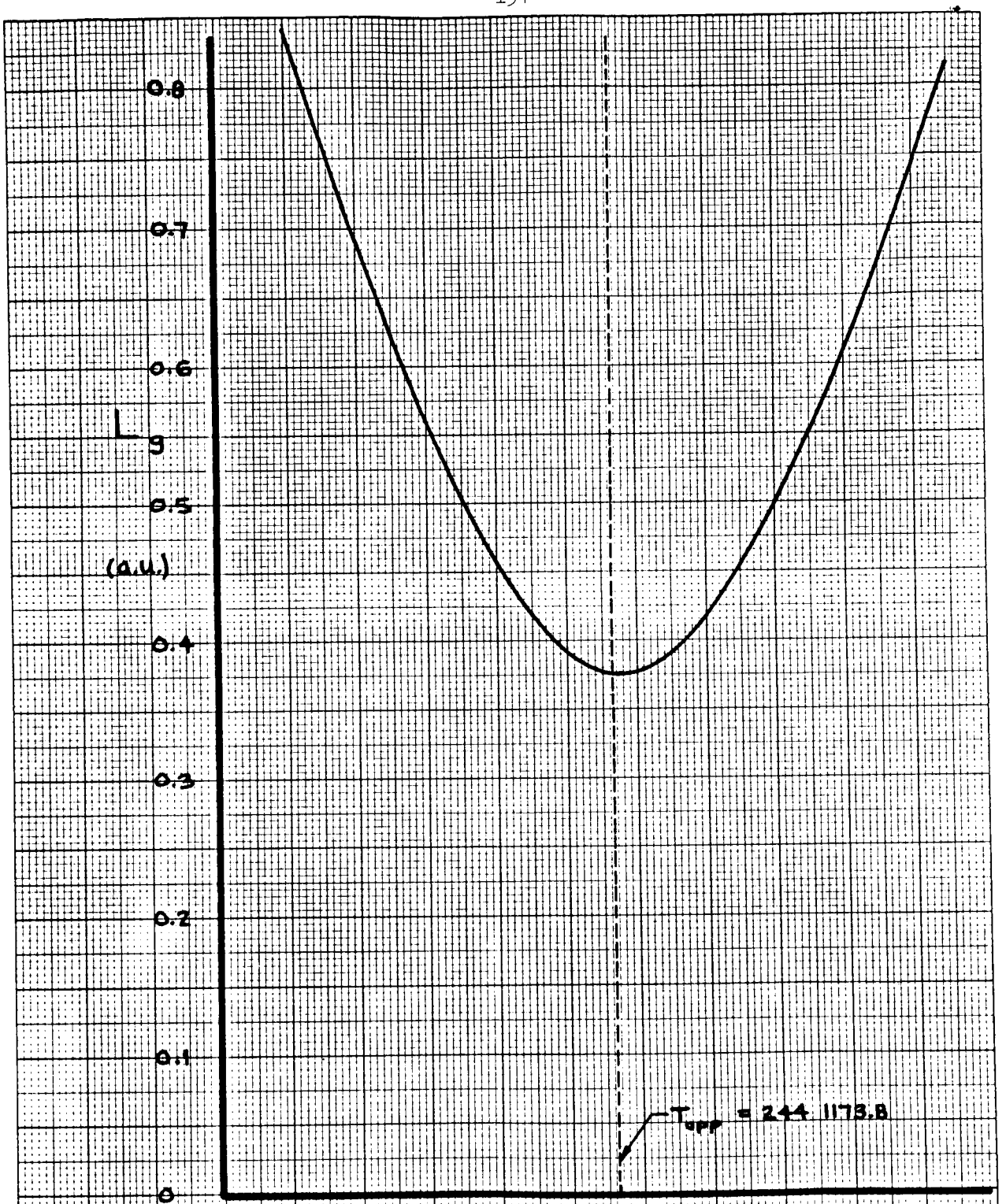

FIG. 17. GEOMETRIC SEPARATION DISTANCE BETWEEN EARTH AND MARS NEAR 1971 OPPOSITION

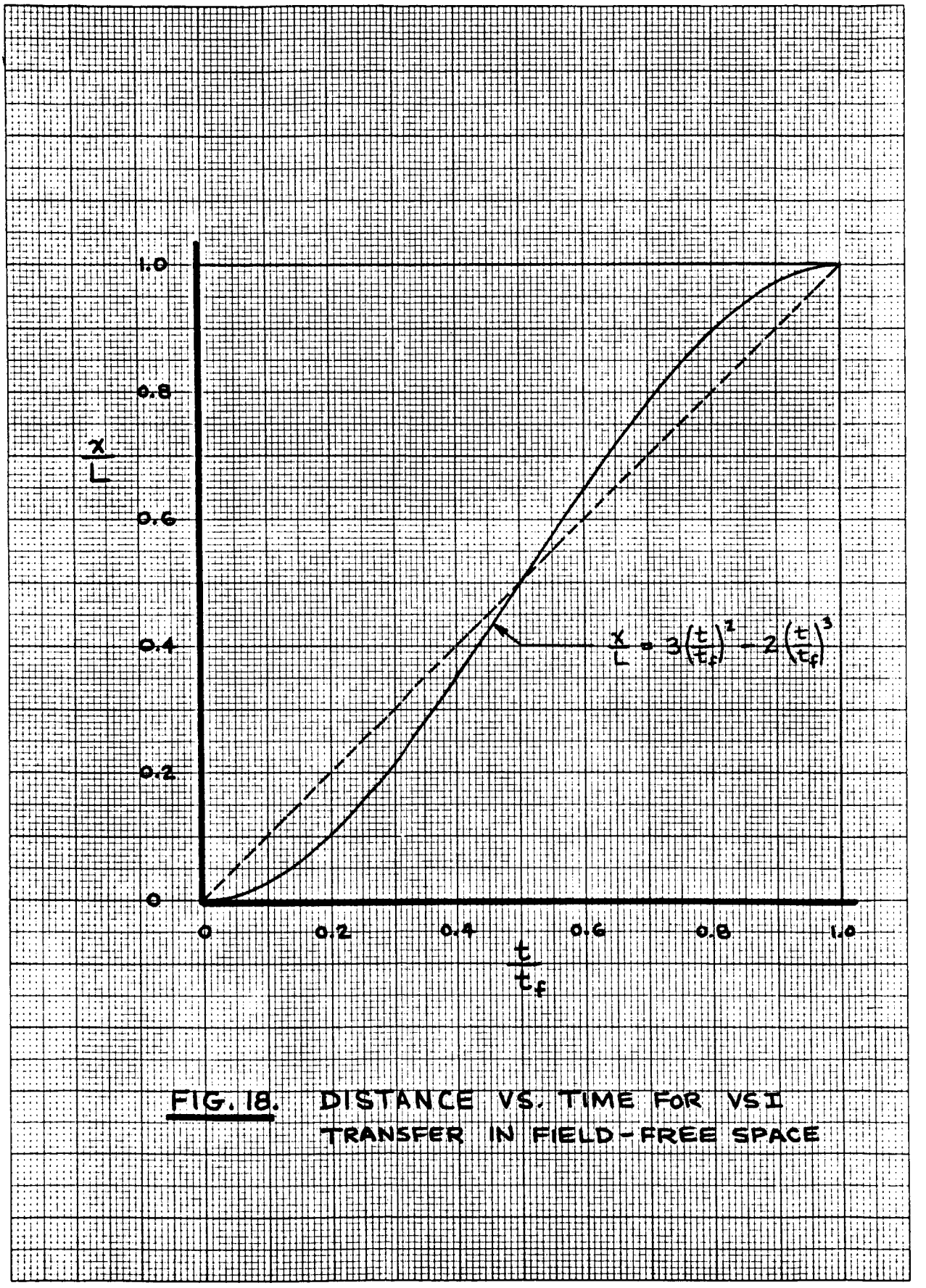

FIG. 18. DISTANCE VS. TIME FOR VSI TRANSFER IN FIELD-FREE SPACE

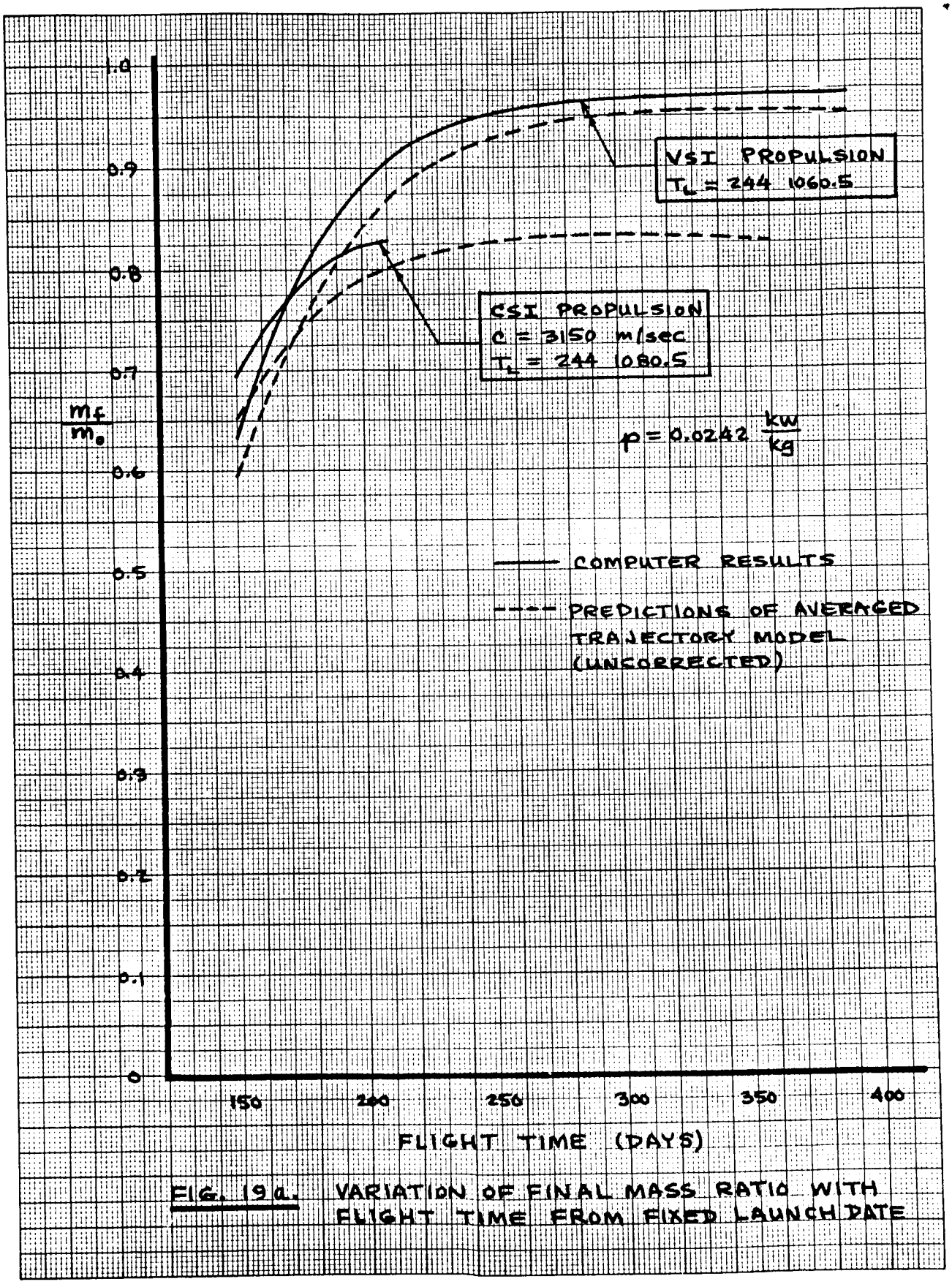

FIG. 19a. VARIATION OF FINAL MASS RATIO WITH FLIGHT TIME FROM FIXED LAUNCH DATE

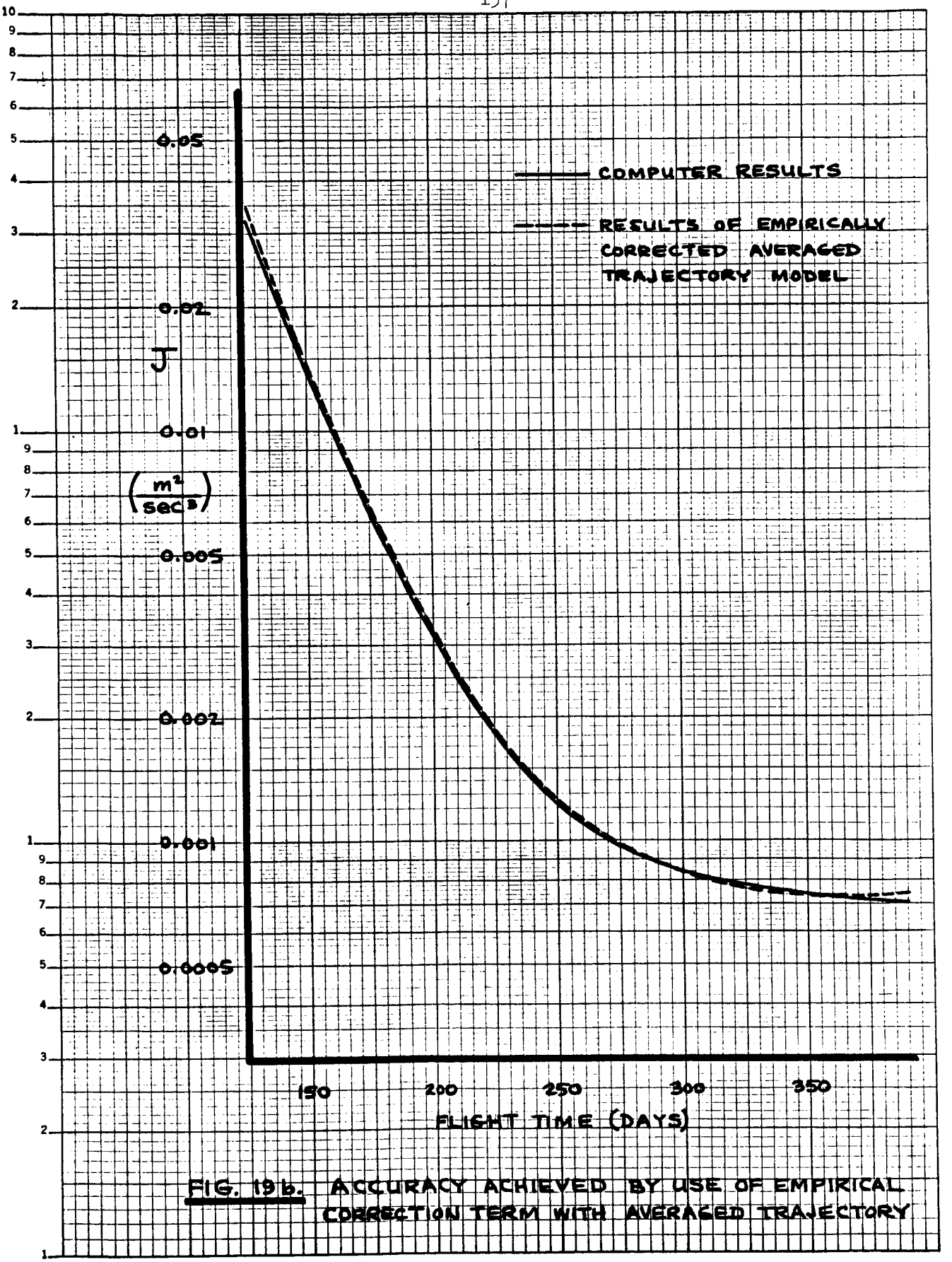

FIG. 19b. ACCURACY ACHIEVED BY USE OF EMPIRICAL CORRECTION TERM WITH AVERAGED TRAJECTORY

Semi-Logarithmic
3 Cycles x 10 to the Inch

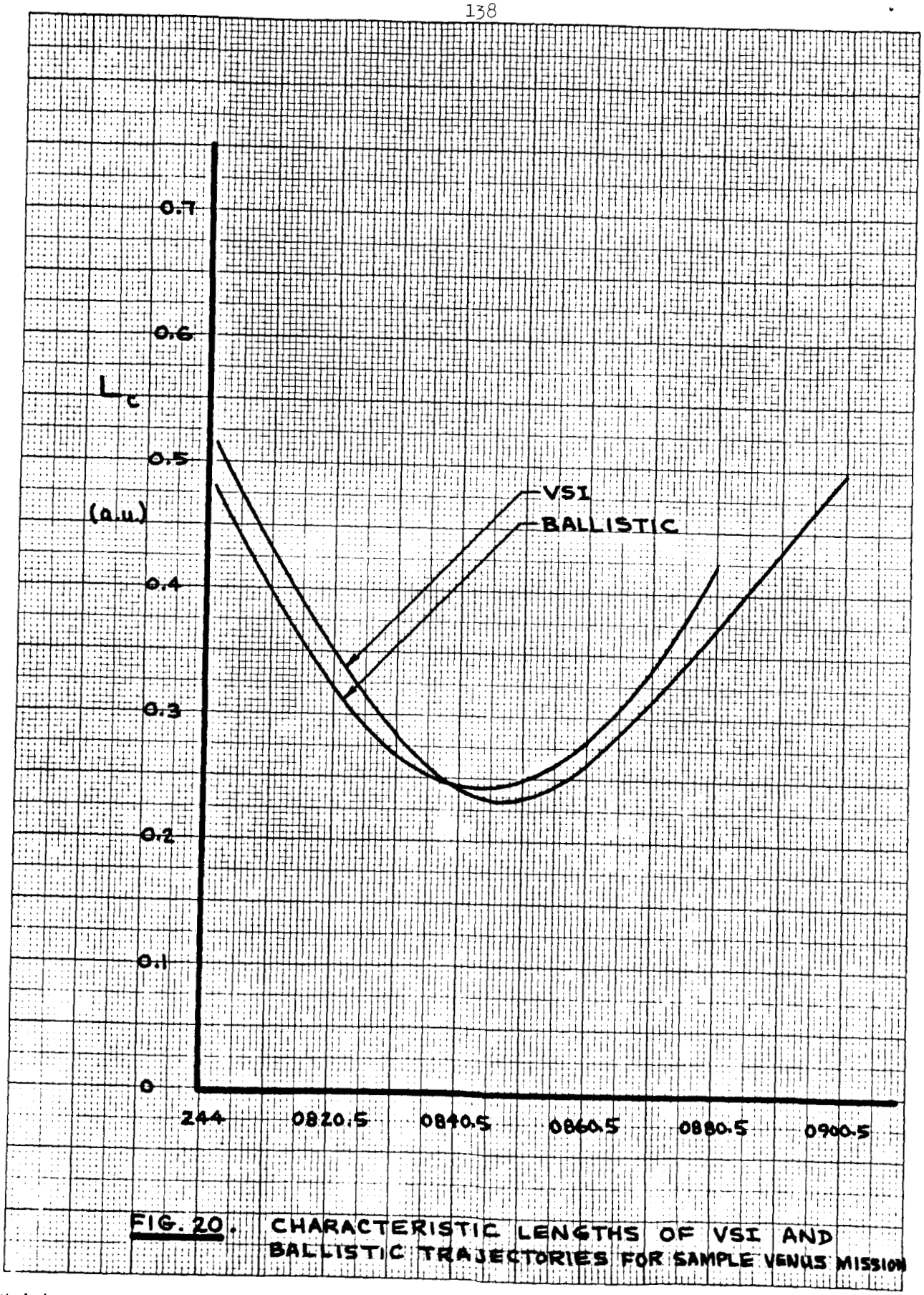

FIG. 20. CHARACTERISTIC LENGTHS OF VSI AND BALLISTIC TRAJECTORIES FOR SAMPLE VENUS MISSION

REFERENCES

1. Melbourne, W. G., "Interplanetary Trajectories and Payload Capabilities of Advanced Propulsion Vehicles," JPL TR 32-68, March, 1961.

2. Edelbaum, T. N., "The Use of High- and Low-Thrust Propulsion in Combination for Space Missions," J. of the Astronautical Sciences, Vol. IX, No. 2 summer 1962.

3. Miele, A., "The Calculus of Variations in Applied Aerodynamics and Flight Mechanics," Chapter 4 of Optimization Techniques, G. Leitmann, ed., Academic Press, New York, 1961.

4. Gobetz, F. W., "Optimal Variable-Thrust Transfer of a Power-Limited Rocket Between Neighboring Circular Orbits," UACRL Report B-110058-10, June 1963.

5. Carlson, N. A., "Optimal Constant-Thrust Transfer Between Adjacent Coplanar Circular Orbits," UACRL Report B-110058-12, November, 1963.

6. Edelbaum, T. N., "Optimum Low-Thrust Transfer Between Circular and Elliptic Orbits," Proceedings of the Fourth U. S. National Congress of Applied Mechanics, ASME, New York.

7. Pontryagin, L. S., "Optimum Control Processes," Automation Express, 1, No. 10, 1959.

8. Kalman, R. E., "The Theory of Optimal Control and the Calculus of Variations," RIAS, Report 61-3, Baltimore, 1961.

9. Breakwell, J. V., "The Optimization of Trajectories," J. Soc. Indust. Appl. Math., Vol. 7, No. 2, June, 1959.

10. Bryson, A. E., and Denham, W. F., "A Steepest Ascent Method for Solving Optimum Programming Problems," Raytheon Co. Report BR 1303, August, 1961.

11. Kelley, H. J., "Method of Gradients," Chapter 6 of Optimization Techniques, G. Leitmann, ed., Academic Press, New York, 1961.

REFERENCES (Cont.)

12. Bellman, R., "On the Determination of Optimal Trajectories Via Dynamic Programming," Chapter 8 of Optimization Techniques, G. Leitmann, ed., Academic Press, New York, 1961.

13. Mitchell, E. D., "Guidance of Low-Thrust Interplanetary Vehicles," Sc. D. thesis, M.I.T., 1963.

14. Melbourne, W. G., and Sauer, C. G. Jr., "Optimum Thrust Programs for Power-Limited Propulsion Systems," JPL TR 32-118, June 1961.

15. Zola, C. L., "Trajectory Methods in Mission Analysis for Low-Thrust Vehicles," AIAA Preprint No. 64-51 of Aerospace Sciences Meeting, New York, Jan. 20-22, 1964.

16. Space Flight Handbooks, Vols. 1-3: Planetary Flight Handbooks, NASA SP-35, Office of Scientific and Technical Information, NASA, Washington, D. C., 1963.

17. Hollister, W. M., "The Mission for a Manned Expedition to Mars," Sc. D. Thesis, M.I.T., 1963.

18. Deerwester, J. M., "Initial Mass Savings Associated with the Venus Swing-by Mode of Mars Round Trips," Paper No. 65-89 of the Second Aerospace Sciences Meeting, New York, January 25-27, 1965.

19. Planetary Coordinates for the Years 1960-1980, Her Majesty's Stationery Office, London, 1958.